01 August 2019

Dr. Eric Lajeunesse
Associate Editor
Earth Surface Dynamics

Dear Eric:

We have made minor edits to the manuscript following the recommendations that Jens, Christian and yourself have made. Thanks for your patience while handling the manuscript and for your feedback. The following pages contain all feedback provided and our reply (***bold italics font***) to each particular point brought up. The 'Track Changes' version of the manuscript is attached at the end of this document. References to page, line in our replies correspond with the 'Track Changes' version.

We look forward to the publication of this manuscript and to future submissions to ESurf.

Sincerely,

Roberto Fernández
On behalf of all authors

ESurf – Round of Reviews No. 2 – Minor Revisions

Associate Editor Decision: Publish subject to minor revisions (review by editor) (20 Jul 2019) by Eric Lajeunesse

Comments to the Author:

Dear Roberto Fernandez,

Thank you for submitting a revised version of your manuscript entitled "Experiments on patterns of alluvial cover and bedrock erosion in a meandering channel" to ESurf. I have received the reports of the two referees. Both of them feel that the manuscript is much improved. Yet they report a detailed list of small issues which need to be resolved before the paper can be published in ESurf. In particular, I regret that several methodological points answered in the rebuttal are not included in the new version of the manuscript.

Thanks Eric. We have added a few more details and relevant references to the supplemental material throughout the text to make sure all information regarding methodological issues is covered. See Sections 2.2, 2.3, 2.4, 2.6.

Reading the new version of the manuscript, I have noted that the logarithmic term log(qs/qbt) in equation (8) diverges when the sediment supply ratio tends towards 0. This prediction, likely inconsistent with Physics, suggests that equation (8) does not describe the small sediment flux limit. If so, this fact should be clarified and discussed carefully. I also recommend you to use a logarithmic scale for the horizontal axis of Figure 5c, as this is the only way to evidence unambiguously a logarithmic dependency of the areal fraction of alluvial cover pc with the sediment supply ratio qs/qbt.

Thanks for pointing this out. We modified figure 5c to include a logarithmic horizontal axis and have included a statement saying that Eq. 8 does not describe the small sediment flux. P10.L1-2. Figure 5.

I encourage you to submit a suitably revised version of your manuscript taking into account the remaining issues raised by the reviewers and myself. Upon submission, we will need to receive a response to reviewer file that lists each of the comments and describes how the manuscript has been modified (or not) in response to those comments.

I look forward to receiving your revised manuscript.

Sincerely yours,

Eric Lajeunesse

Reviewer 1 – Jens Turowski

Dear authors:

Thanks for the revised manuscript. I read it with interest. The paper is somewhat improved and the methods are largely clear now. Nevertheless, I still find inaccuracies especially in the introduction, and the research gap and aims are not cleanly set up. The material presented in the introduction needs to be focused and stream-lined.

I appreciate that you picked up some of my previous suggestions in the discussion. Yet, I am a little surprised that some of the most obvious similarities are glanced over. As an example, in the Turowski and Hodge paper, we derive a cover equation with a logarithmic shape somewhat similar to what you fit to the experimental data (see eq. 27 and 31 in that paper). I wonder why this is not discussed.

There is also a mixture of discussion material in the results. Please look out for this and move / rewrite accordingly. I might have overlooked something, but it seems to me that some of the methodological points were answered in the rebuttal, but didn't make their way into the manuscript (e.g., properties of the cement, asked both by me and Christian Braudrick). Please review and amend this.

Finally, the 6 points in the conclusion do not directly pertain to the four points that are said to be addressed by the study at the end of the introduction. It would be good to rewrite this to have a direct relationship.

Thanks Jens. We have made edits to the manuscript following your recommendations. Specific aspects are mentioned below. To answer your general concerns:

- ***We are happy with the introduction we have written.***
- ***We have added an explicit reference to Eqs. 27 and 31 in Turowski and Hodge(2017) where we introduce Eq. 8 in our manuscript.***
- ***We have moved the 'discussion material' to the discussion and changed the order of the three last figures (and references to them in the text).***
- ***Our 6 conclusions pertain to all four points in the introduction. Some conclusions pertain to more than a single aspect in the introduction. It was not our objective to provide a single conclusion per issue raised in the introduction.***

2.8 …Gilbert did not specifically use…

We removed the year. P2L8

2.14 only the 2001 paper includes experimental work

We removed the 1998 reference. P2L14

2.15 The description here relates just to the cover effect. The tools effect is parameterized as a linear dependence on sediment supply in the saltation-abrasion model.

We edited the paragraph to indicate this. P2.15-17

2.16 The saltation-abrasion model…

We have made this edit. P2.L17

2.25 Lague's model is not for bedrock incision, but for bedrock channel morphodynamics

We have made this clarification. P2.L26.

2.26 Misleading: his cover model is equivalent as described, the context suggests that you mean the morphodynamics model.

We have made this clarification. P2.L27

2.28 and following: the paragraph features a string of loosely connected statement (jumping from a brief description of Zhang's cover model, to Turowski's 1D model of steady state channel morphology to Mishra's experiments) and lacks a clear line of argument. The references are treated at different level of detail; a symmetry is lacking. The point of the introduction should not be to list all previous cover models and their applications, but provide an argument that leads to the research gap and question.

We provide a more detailed description of recent advances because they are relevant to our work. We then say that even these advances are lacking certain aspects and introduce our research questions.

3.4-5 I somewhat disagree with this statement of the research gap, because in my mind it confounds two unconnected problems. Let me explain this briefly. When we think about cover, we have two problems to solve. Consider a particular control area on the bed (in a discrete model, this would be a pixel, in a continuous formulation an infinitesimal area element). 1) For a given amount of sediment mass or volume, we need to know how this is distributed to give a particular cover fraction. As a concrete example, if we have, say, 1/100 of a cubic meter of sediment deposited on an area of 1m2, we could have a complete cover of 1cm thickness of the entire area, or we could cover half of the area by a 2cm thick layer. Or there are an infinity of other possibilities to distribute this sediment. Therefore, we need a relationship between cover fraction and sediment mass (or volume). The point of the exponential cover function of Turowski et al. 2007 and Turowski 2009, and of the P function of Turowski and Hodge 2017 is to provide such a relationship. 2) We need to know how much sediment deposits in a given area element (the total mass or volume per area element of the bed). This is done by relating deposition and erosion to hydraulics. In general, this is done either using a framework based on the Exner equation (e.g. Zhang's or Inoue's work) or on the entrainment-deposition framework (e.g., Turowski and Hodge 2017, Shobe et al. 2017).

We don't understand the difference between 1) and 2). If you know how a given mass of sediment is distributed over a bed area, leading to a cover fraction (point 1) you immediately know how much sediment deposits in a given area element (point 2**). How are these different/unconnected? Perhaps we can discuss this further when we cross paths.**

3.7 There is also earlier work by Nelson and Seminara (2011 and 2012).

We have added the references to their work. P2.L4, P2.L9

3.8 Again, here is a confusion between morpho-dynamic models and models of bedrock incision. As an example, the saltation-abrasion model is a model of bedrock incision; it predicts erosion rate (that is volume removed per time and per bed area) as a function of hydraulics, and sediment properties and transport rate. It has been used in 0D/1D morphodynamics models for example by Sklar and Dietrich 2006, by Zhang et al., or by Turowski 2018. Similarly, the stream power / shear-stress model is a bedrock incision model, which has been used in a number of morphodynamics frameworks (e.g., Wobus et al. 2006, Stark, 2006).

We have added 'morphodynamics models' to clarify. P3.L9-10

3.9-11 What about the experiments by Friedl (chapter 7 of https://www.ethz.ch/content/dam/ethz/special-interest/baug/vaw/vaw-dam/documents/das-institut/mitteilungen/2010-2019/245.pdf, mentioned in one of my previous comments)?

The experiments of Friedl look at the effects of sediment supply over an armoured bed. Although there are connections between the cover patterns seen therein and our work, their focus was not on the cover effect. The citations we included in this paragraph are specific to the cover effect in bedrock rivers.

3.10 I still think the formulation is misleading. The reply in the rebuttal does not convince me (it is not the assumption of the model that sediment can only be transport on covered parts of the bed). Maybe it would be good if you make the assumptions underlying your interpretation of the model explicit, and more clearly explain your line of thinking.

Line 4.10.

If the transport capacity corresponds to a fully alluviated bed, the term qbs = pc*qbt implies that sediment transported in the reach is only available in those areas of the bed that are covered with sediment. It doesn't imply that sediment is only transported over covered parts but rather that sediment can only be mobilized from alluviated areas.

P4.L10

3.13 Maybe it would be helpful to define 'throughput load' here.

Line 4.13.

We have added a definition. P.4L13-14.

3.14 Again, this is inaccurate. Yes, some models, notably the linear cover model, are based on temporally representative values (essentially using long-term 'effective' values for hydraulics and sediment supply). Still, sediment supply and transport capacity could be written as functions of time. In that way, one can model temporally evolving cover. This approach neglects the response time of cover to changing conditions, i.e., cover is always adjusted to the boundary conditions and any lags are neglected. The mass/volume based formulations are more general, one could write mass/volume as a function of time. The crux is to couple these cover models to proper hydraulic and sediment transport models. And even this has been done in a handful of papers (most of which you cite earlier). Finally, in the Turowski and Hodge 2017, we devoted an entire section to response time scales, including analytical solutions and explicit formulations of response time scales, and a discussion of leads and lags, going far beyond the 'loose definition' that you claim to exist to date. Regarding the spatial time scale, there are papers that upscale from the grain scale (which I already pointed out in the last round of reviews). Again, here the problem is related to appropriate length scales of hydraulics, rather than cover.

We have changed 'only loose' to 'different'. P3. L16

3.17 I still think you need to supply a clear definition of what you mean by transient cover.

We decided to leave this open on purpose and then discuss the issue in section 4.1.

3.20-24 Again, I point to the Turowski and Hodge paper. The model provided therein for sediment transport is physically based and can deal with temporal cover fluctuations (see their figures 10, 11 for examples of temporal evolution of cover in generic situations and 14 for an example calculation

for a real flood event). Another model (that I did not mention in my previous review) is the one of Johnson, JGR 2014. He deals with feedbacks between cover and bed roughness.

We have edited the text and now it says that 'physical measurements' as opposed to 'physically based approaches'. P3.L24.

3.25 From an experimental point of view the question is fair. However, I suggest to state that there are models that predict a much wider range of behaviors. See for example the cellular automaton of Hodge and Hoey 2012 or the simulations of Aubert et al. (ESurf 2016). The P-function framework of Turowski and Hodge is sufficiently flexible to be able to describe all of these observations.

We have edited the text to include this observation. P3. L26, 28, 29-30.

3.28 It has also been shown to not be an acceptable approximation in previous work (incidently, also in some of the cases described in the cited paper).

That is why the text said 'different circumstances' not 'all'. We edited to 'certain circumstances' to avoid confusion. P3. L28

4.7 why 'alternative'? The saltation-abrasion model evaluates to the same equation (2) once all the terms in (1) are evaluated. We do not show how Eq. (1) becomes Eq. (2).

We ***have removed 'alternative' and just call it a closely related equation. P4. L6-7***

4.13 I do not see this readily. If we view p_0 and p_c as a function of time and space, the equation is still valid. (And this is exactly what is done in the following paragraph.) See also my comment to 3.14.

The argument being made is about the values of pc and po which will always be zero or one in the case of throughput bedload. Even if you average in space and/or time, the bed will never have alluvial cover deposits for as long as the bedload enters and leaves the reach without depositing (i.e. particles continuously saltate, roll or slide).

4.14 Full stop instead of comma after sense.

Thanks, this was a typo. We have edited it. P4.L11.

4.15 grammar / sentence unclear (P_0 is this but instead that).

We have edited the text slightly to improve readability. P4.L16, L17.

14.12 Slightly inaccurate; the assumption is of uniformity within the area of consideration. One could divide the bed in multiple cells where this assumption is (approximately) valid and in this way model cross-stream variations.

Although in my previous papers, I have dealt with a control area with homogenous conditions, it would be straight-forward to expand this to full 2D models, by placing a number of homogenous control areas in the long- and in the cross channel direction (building up a grid that represents the bed). Then, the only thing that needs to be added is the long- and cross-stream sediment mass balance as a function of hydraulics, i.e., we need to specify how much sediment moves from a given cell into the neighboring cells. This is straight-forward (though not necessarily easy) because the tools to do this are available (for example, the Nelson and Seminara papers, or other work that deals with 2D resolved sediment transport in alluvial rivers). The question again becomes of how large/small can the considered cells become. We want to make them as small as possible to properly

resolve the hydraulic variations, but large enough so that numerical computations are feasible, and that we can treat sediment as a continuous mass and do not need to deal with granular effects.

We have modified 'channel width' to 'considered area of unspecified dimensions'. P15.L3-4

4.19 It is not an arbitrary function. 'Arbitrary' means that it does not matter which function is chosen. Instead, there are some clear constraints on the function, both from fundamental logic / definitions (i.e., cover cannot be smaller than 0) and from observations.

We have removed the word 'arbitrary'. P4.L20

4.20 What are your arguments to judge this as the 'simplest realistic form'? What observations does your realism hang on? Not sure whether I would call a discontinuous function realistic…

We have edited the text and refer to them as 'commonly used functions'. P4.L21

4.27 The statement '…and channel geometry would not change over time' does not follow from what has been said before. Clearly, channel morphology changes if, say, only the right side of the channel bed erodes and not the left side. I would even argue the other way round: as long as there is erosion somewhere (partially covered bed) persistent cover necessarily leads to an adjustment of channel geometry!

If pc = 0 or pc = 1 erosion would always be zero according to the relations presented above. Therefore, channel geometry would indeed not change in time.

4.28 Again, this is not necessarily true. You may have patches of cover moving through and still adjust the channel (for example if wall erosion rates are much high than bed erosion rates). This is because erosion rate is not only dependent on the cover effect, but also on the tools effect (tools concentration may vary, as may the impact rate for a given concentration, or there may be a lateral sorting of grain sizes).

We changed 'cross section' to reach and added a reference to Sklar and Dietrich to avoid confusion. P4. L28-30.

5.1 Better: may form – not all meander bends necessarily have point bars at all times. Also consider temporal variation of floods – we do not really know whether point bars persist throughout the largest floods.

We have added the word 'may'. Thanks for this observation. P5.L1.

5.2 …breaks down…

Refers to assumptions. 'break down' is correct.

5.18 What point cloud?

It referred to the bathymetry. We have edited the text to make it clear. P5.L17-18.

5.31 The term macro-roughness appears here for the first time pertaining to the experiment. What do you mean by it?

We have added our definition of bedrock macro-roughness when it appeared for the second time… Thanks for pointing this out. We have moved the definition to this paragraph. P.5.L31.

9.20 Eq. (8) – compare to the results of Turowski and Hodge, e.g., eq. 27 and 31 in their paper. This gives a similar logarithmic function in the cover domain, where the exponential term is approximately zero.

We have added a reference to this paper and the specific equations. P10.L1-3.

Aubert et al. (ESurf 2016) also predict a similar function from their models.

We also added a reference to this paper. P10.L3-4

9.31 I am still not convinced by the use of the logistic curve. For qs/qt=0, this gives finite cover, which is unphysical. It is not difficult to find an equation that honors that condition and otherwise has similar poperties.

We have made a clarification on this regard. The model of Zhang et al (2018, 2015) and others based on it (e.g. Inoue and colleagues) use the alluvial cover to macro-roughness ratio between a characteristically low (e.g. 0.05) and a characteristically high (e.g. 0.95) value to avoid singularities or unphysical results. P10.L23-24.

11.30 this is an interpretation that should be placed into the discussion section

We have moved it to the discussion. P15.L20-21, 24-26.

13.12-26 this is discussion material

Idem. P16.L30-31 and P17.L1-15.

13.31-14.3 discussion material

We left this here because it actually serves as the transition point between the results and discussion section.

14.28 no comma after 'above'

This was a typo. We have removed the comma. P15.L19.

16.7 ...and Nelson and Seminara 2011

Yes! We have added this reference. P17.L23

17.2 They showed that energy can transferred, not that erosion is possible. Erosion was not investigated in this study.

Thanks. We have edited the wording and mention energy instead of erosion. P18.L18-19

17.15 citation incorrect, should be Turowski and Hodge 2017.

Thanks. We have modified it. P18.L32

Reviewer 2 – Christian Braudrick

The paper by Fernandez et al reports on a very interesting set of experiments exploring bedrock erosion in a sinuous channel. Their novel approach and clever measurements make this paper a crucial addition to the bedrock erosion literature. The videos that will be included in the SI are fascinating. Several notable findings, including that the areas of transient and permanent cover were of similar magnitude will be useful to develop a bedrock erosion theory for sinuous channels. The authors responded to the previous comments including fixing the structure of the paper, beefing up some of their citations as pointed out by Jens, and addressed minor comments throughout the document. The comments below are very minor, and I do not think another review would be necessary once these comments are addressed.

The details about the transition between experiments were include in the response to comments, but not included in the revised paper or SI that I could see. To avoid any confusion, I think those details should be included in the methods section.

We have added more details regarding the transition between runs and more references to the supplemental material to make sure that the methods are clear. P7.L26-27, L30-31, P8.L1-2.

A sentence or two about the resolution of the camera in the SI or paper would be helpful.

We added this information in section 2.4. P6. L21-24

Page 6. The discussion of the polynomial in the SI was clarifying and the SI should be referenced in the text where the polynomial was discussed.

We have added the reference to the supplemental material. P6.L8-9.

Page 6, Line 20. A sentence about the pixel size of the camera would be helpful to interpret the results. If the pixel size is larger than the particle than the bed Presumably particles are mostly grouped, was the threshold to detect the presence of sediment set to pick up if a single particle fell into the pixel or is it likely that more than a single particle was necessary for Matlab to record the point as containing sediment? This may not matter since it sounds like the particles were moving in bedforms, but it might be worth addressing, and least in the SI.

We added this information in section 2.4. P6.L21-24.

Page 7, Line 7 and Figure 5a,b. Shouldn't figures 5a and 5b have two sets of data on them since the experiments were repeated? I am very surprised that the experiments were so repeatable. I think the authors misunderstood Jens' comments about human error. The most likely sources of human error are evenly distributing the particles.

We have added both sets of data (circles and squares in Figs. 5a, 5b). See figure 5.

Page 8 Line 6, Figure 2 shows that the bedload trap is downstream not upstream.

We have clarified the text. P.8.L20-21.

Page 9. The organizational issues have mostly been dealt with, with the exception of the description of figure 6 in Lines 11-14, which comes between the description of Figure 5 and the discussion of Figure 5.

We have moved the paragraph following this recommendation. Thanks. P11.L1-4.

Page 10. Equations 9 and 10. These equations feel like the should come before the previous paragraph to be immediately below the paragraph that describes them.

We have moved the equations following this recommendation. Thanks. P10.L20-21

Page 11 and Figure 10. I spent a lot of time thinking about this figure and the discussion in the text. I wondered whether the small increases and decreases in persistent and transient cover were repeatable or if they were just scatter in the data. I think its just as likely that its scatter as it is due to a trend in the data. Another explanation is that equilibrium had yet to be reached when the data recording began. Figure 7 shows that the cover varied temporally in Pc=0.78, 0.72, 0.46, 0.38, and 0.27 (where there was a increasing cover trend). It is really interesting that the persistently covered area and transiently covered area are similar. What a cool finding.

We definitely need to look at a lot of data not included in this manuscript which relates to the conditions between one state and another. We also have data for hours and hours of the same run which would allow determining if it's scatter or a trend.

Page 11, Line 20. Why would the depth be constant? If the slope and roughness are changing you would think that the depth and velocity would adjust. I don't recall water surface (or velocity) measurements. If the slope is changing isn't the depth changing too?

We have adjusted the text to clarify this point. The no-flow water depth was kept constant but it certainly changes based on the amount of sediment in the flume and the percent of cover. The water surface slope changed accordingly. We have a paper in review in JHR looking at the instantaneous water surface elevation changes based on the eTape readings as alluvial cover changes in the flume. P12.L11-13.

Page 15, bottom. Did the authors observe particles striking the bank, or is that inferred?

This is inferred. We introduce this set of arguments with 'Our results suggest'. P16.L27.

Page 16, Lines 21-26. Presumably the distribution of the grain size and roughness matter too, which would likely be larger in the field? Also, there is a lot in "hydraulic conditions".

We edited the text to include 'grain size'. Agreed. P18.L7.

Table 2. Inferring the middle reach slopes for pc54-79 to two decimal points seems like too much. It is hard to justify 2 decimal points, and looking at the table, it seems like there would be a lot of scatter in the relationship between overall slope and middle bend slope. The more I think about this the more I think they shouldn't be included at all. The slope measurement with two local data points is probably not very robust anyway.

We removed a decimal point. Table 2.

Experiments on patterns of alluvial cover and bedrock erosion in a meandering channel

Roberto Fernández[1], Gary Parker[1, 2], Colin P. Stark[3]

[1]Ven Te Chow Hydrosystems Laboratory, Department of Civil and Environmental Engineering, University of Illinois at Urbana-Champaign, Urbana, IL 61801, USA
[2]Department of Geology, University of Illinois at Urbana-Champaign, Urbana, IL 61801, USA
[3]Lamont Doherty Earth Observatory, Columbia University, Palisades, NY 10964, USA

Correspondence to: Roberto Fernández (fernan25@illinois.edu)

Abstract.

In bedrock rivers, erosion by abrasion is driven by sediment particles that strike bare bedrock while traveling downstream with the flow. If the sediment particles settle and form an alluvial cover, this mode of erosion is impeded by the protection offered by the grains themselves. Channel erosion by abrasion is therefore related to the amount and pattern of alluvial cover, which are functions of sediment load and hydraulic conditions, and which in turn are functions of channel geometry, slope and sinuosity. This study presents the results of alluvial cover experiments conducted in a meandering channel flume of high fixed sinuosity. Maps of quasi-instantaneous alluvial cover were generated from time-lapse imaging of flows under a range of below-capacity bedload conditions. These maps were used to infer patterns of particle impact frequency and likely abrasion rates. Results from eight such experiments suggest that: (i) abrasion through sediment particle impacts is driven by fluctuations in alluvial cover due to the movement of freely-migrating bars; (ii) patterns of potential erosion are functions of sediment load and local curvature; (iii) low sediment supply ratios are associated with regions of potential erosion located closer to the inner bank, but this region moves toward the outer bank as sediment supply increases; and (iv) the threads of high erosion rates are located at the toe of the alluvial bars, just where the alluvial cover reaches an optimum for abrasion.

1 Introduction

In his report on the geology of the Henry Mountains, Gilbert (1877) advocated that the process of mechanical erosion of a bedrock river bed by material transported by the current depends on the hardness of the bedrock, the hardness, size and number of particles in transport, and the velocity of the stream. He noted that the number of sediment particles striking the bed and eroding it could increase up to the sediment transport capacity of the stream. At this point, the bed would be so crowded with particles that instead of colliding against the bed, they would collide against each other and the bedrock would be protected from erosion. Based on this observation, Gilbert (1877) stated that it is probable that the maximum work of mechanical erosion is performed when the load is far below the transport capacity of the stream.

During the last two decades, particular attention to the previously-described phenomenon has motivated experimental (e.g. Mishra et al., 2018; Hodge et al., 2016; Hodge and Hoey, 2016; Johnson and Whipple, 2010, 2007; Chatanantavet and Parker, 2008; Finnegan et al. 2007; Sklar and Dietrich, 1998), theoretical or numerical (e.g. Turowski 2018; Turowski and Hodge, 2017; Zhang et al. 2015; Inoue et al. 2014; Johnson 2014; Nelson et al. 2014; Nelson and Seminara, 2012; 2011; Lague, 2010; Chatanantavet and Parker, 2009; Turowski et al., 2007; Whipple et al., 2000), and field (e.g. Ferguson et al., 2017; Beer et al. 2017, 2016; Beer and Turowski, 2015; Johnson and Finnegan, 2015; Inoue et al. 2014; Cook et al., 2013, 2009; Hodge et al., 2011) work examining the relation between sediment supply, degree of alluviation, and bedrock incision in mixed bedrock-alluvial rivers. Although Gilbert ~~(1877)~~ did not specifically used the terms 'tools' and 'cover' effects, he described them vividly. Saltating bedload particles in a bedrock river are one of the 'tools' needed to cause incision. As sediment supply increases to a river reach, the ability to incise eventually decays due to the appearance of sediment deposits which protect the bed from further abrasion ('cover' effect). Therefore, in order for bedrock erosion to occur, a balance must exist between the 'cover' and 'tools' effects such that there are enough sediment particles in the system striking the bed, but not so many as to cover it and protect it from abrasion.

The experimental work of Sklar and Dietrich (2001~~, 1998~~) has led to a better understanding of the 'tools' and 'cover' effects. In their work, the ~~'tools' and~~ 'cover' effect~~s were~~ was parameterized in terms of a cover factor p_c which represents the areal fraction of bedrock that is covered by sediment. The exposed fraction is thus defined as $p_o = 1 - p_c$. The tools effect was parameterized as a linear dependence on sediment supply. The ~~cover~~ saltation-abrasion model of Sklar and Dietrich (2004) was the first to include these effects in a bedrock erosion model. The cover model used by Sklar and Dietrich (2006, 2004) to compute erosion linearly relates the areal fraction of the bed that is covered by sediment to the ratio of sediment supply to sediment transport capacity of a bed fully covered with alluvium. The linear cover model has under certain conditions been validated via experimentation (e.g. Chatanantavet and Parker, 2008; Finnegan et al., 2007; Johnson and Whipple, 2010, 2007). Turowski et al. (2007) proposed an exponential cover model, which assumes that at below capacity transport conditions, sediment grains have equal probability of forming deposits over any part of the bed and cover could be static (immobile sediment) or dynamic (mobile sediment but still protects the bed from abrasion due to grain-grain interactions). Turowski and Rickenmann (2009), using a piezoelectric bedload sensor, show some field evidence for the dynamic effect in the Pitzbach in Austria. Lague (2010) also proposed a bedrock ~~incision~~ channel morphodynamics model based on stochastic variations of discharge and sediment supply which accounts for alluvial thickness and its effect on limiting bedrock incision. His cover model is equivalent to the former two when working with the mean sediment thickness.

Recently Zhang et al. (2018, 2015) proposed the macro-roughness saltation-abrasion alluviation model which treats the cover factor as the ratio between the alluvial thickness at a river cross section to the characteristic macro-roughness height of the bedrock surface. The advantages of this approach over the ones previously described is that by relating cover to alluvial thickness rather than sediment supply, it can deal with waves of alluviation and bed stripping and their dynamic effect on incision or the cessation thereof due to complete alluvial cover. Turowski (2018) presented a model that links alluvial cover to the width, slope and sinuosity of mixed bedrock alluvial rivers and postulates that change in channel width and sinuosity

over time depends only on the amount of alluvial bed cover. Finally, Mishra et al. (2018) conducted experiments in a U-shaped meandering channel with constant curvature and showed that: i) lateral erosion increases with sediment supply ratio, ii) vertical incision initially grows with sediment supply but shows a more complex relation due to the interplay between bedrock erosion and sediment deposition, and iii) zones of erosion along the toe of the point bar result in the formation of outer bedrock benches.

In spite of these developments, the cover factor definitions used so far by the different authors lack one or more important aspects required for the development of a model of bedrock incision in mixed bedrock-alluvial meandering rivers, namely:

(i) What are the roles of sediment supply and local curvature and how do they affect the areas of potential erosion in meandering bedrock-alluvial channels? With the exception of the recent work by Mishra et al. (2018), Inoue et al. (2017, 2016), ~~and~~ Nelson et al. (2014), and Nelson and Seminara (2012), all models of bedrock incision by abrasion, or morphodynamics of mixed bedrock-alluvial rivers ~~are~~ are either '0D' or '1D' and most experiments have been conducted in straight channels (e.g. Johnson and Whipple, 2010, 2007; Chatanantavet and Parker, 2008; Finnegan et al., 2007). Even though Shepherd (1972) and Shepherd and Schumm (1974) did experiments with alluvial cover in bedrock analog substrates and report on erosion patterns in mixed bedrock-alluvial channels with some sinuosity, there is still no baseline set of experiments describing how the pattern of spatial cover is established in a meandering channel, and how it varies with local curvature and sediment supply.

(ii) What is the appropriate averaging window to characterize the areal fraction of alluvial cover? The model based on the areal fraction of cover uses an average value defined over an "appropriate" averaging window, but ~~only loose~~different definitions regarding its length scale and timescale have been provided to date. Moreover, this mean cover value assumes that the alluvial deposits covering the bed are transient. Field observations (Inoue et al. 2014, Cook et al. 2013, 2009) and laboratory experiments (Johnson and Whipple, 2010, 2007; Chatanantavet and Parker, 2008; Finnegan et al., 2007) indicate that zones of persistent cover and persistent exposure coexist with transient deposits in mixed bedrock-alluvial rivers.

(iii) What is the role of alluvial cover fluctuations on erosion? Current models rely on a mean cover value, but temporal alluvial cover fluctuations provide a better representation of the frequency of the saltating bedload particle impacts on the bed which are responsible for bedrock erosion. Some authors have addressed this issue with probabilistic frameworks (e.g. Turowski and Hodge, 2017; Lague, 2010; Turowski, 2009) but physical measurements ~~ly based approaches~~ are still lacking and experimental data is required for development and validation purposes.

(iv) What is the relation between alluvial cover and sediment supply? Most ~~A~~available models typically treat the relation between sediment supply and areal extent of alluvial cover by using a linear function. This relation has prevailed due to its simplicity and because it has been shown to be an acceptable approximation under ~~different~~ certain circumstances (e.g. Chatanantavet and Parker, 2008). Nevertheless, there are models that predict a much wider range of behaviors (e.g. Turowski and Hodge, 2017; Hodge and Hoey, 2012).

We addressed these questions by conducting experiments in a high-amplitude laboratory meandering flume to characterize the statistics of alluvial cover as they relate to the sediment supply ratio and local curvature. We also addressed the fourth question by conducting a simple experiment on a flat (non-sloping) bedrock slab. Before describing our experimental methods, we present the relevant definitions needed for our analysis.

1.1 Bedrock erosion and alluvial cover

The time rate of bedrock incision (erosion) by mechanical wear E_s has been quantified with Eq. 1 by different authors (e.g. Sklar and Dietrich, 2004, 2006; Turowski et al., 2007; Chatanantavet and Parker, 2009) as follows;

(1)

In Eq. 1, is the volume of bedrock lost per particle impact, is the particle impact rate per unit area per unit time and is the fraction of exposed bedrock. The areal fraction of alluvial cover, i.e. cover factor is thus defined as . A~~n alternative but~~ closely related equation to compute erosion is presented in Eq. 2 (e.g. Turowski et al., 2008; Chatanantavet and Parker, 2009). Let = a parameter that relates to the fraction of bedrock volume that is lost per particle impact at the end of each saltation, - the capacity bedload transport rate per unit width for a bed fully covered with alluvium, and - the actual bedload transport rate per unit width assuming that particles can only be ~~transported~~ mobilized from those portions of the bed that have an alluvial cover. Then.

(2)

But it is readily seen that the above relation breaks down for throughput load, bedload transport which enters and leaves a reach without depositing on the bed and~~, which~~ does not contribute to cover in any meaningful sense.~~,~~ In Sklar and Dietrich (2004) and other works based on their cover model (e.g. Turowski et al., 2007; Lamb et al., 2008), represents the areal fraction of exposed bedrock and is related to the sediment supply ratio (Eq. 3). In the Zhang et al. (2015) cover model, represents the fraction of bed elevation at a given cross section which is not covered by alluvium, ~~but~~ and is instead related to the ratio , where is a measure of the thickness of alluvium, and is a measure of the intrinsic macro-roughness height of the bedrock surface itself (Eq. 4).

Both definitions are presented schematically in Figure 1. In general, is a~~n arbitrary~~ function of or , ~~but~~and ~~the simplest realistic~~commonly used forms are given by Eq. 3 and Eq. 4.

(3)

(4)

Eq. 3 or Eq. 4 in combination with Eq. 1 must be employed in terms of an appropriate averaging window over which to determine the cover fraction and open fraction . For example, Sklar and Dietrich (2006), Gasparini et al. (2007) and Chatanantavet and Parker (2008) assume, explicitly or implicitly, that a) the averaging window is at least as large as channel width, and b) that fluctuates temporally between 0 and 1 within the window. If this were not the case, zones ~~within the channel~~along the reach where persistently takes the values 0 and 1 would never be subject to incision, and channel geometry would not change over time in those reaches. However, if these assumptions are met over an appropriate time scale, all the reach~~channel along a cross-section~~ would, in the long-term average, erode at the same rate (Sklar and Dietrich, 2004).

In the case of mixed bedrock-alluvial meandering rivers, where persistent alluvium deposits may form in e.g. point bars, the assumptions just described break down. In such rivers, erosion occurs only in areas with transient cover and is not expected to occur in areas that are persistently covered or exposed. Under certain conditions, specific areas of the channel might have little to no probability of being struck by sediment particles, thus limiting the areas that could undergo erosion.

2 Materials and Methods

2.1 Flume

Experiments were conducted in the Kinoshita Flume at the Ven Te Chow Hydrosystems Laboratory, University of Illinois at Urbana-Champaign. The flume, shown in Fig. 2b, is 0.60 m wide, 0.40 m deep and 33 m long (along the centerline, not including upstream and downstream tanks), and has a sinuosity of 3.7. All three meander bends are identical and have a down-channel wavelength of 10 m. All results presented herein correspond to experiments conducted with water flowing from right to left as indicated in Fig. 2c, i.e. with the bends skewed in the upstream direction. The flume is a closed system in which water and sediment are recirculated. Readers interested in more specific details about the Kinoshita flume are referred to Abad and Garcia (2009a, b).

2.2 Bed-material properties and bed characteristics

The alluvium used in the experiments was crushed walnut shells, which have a specific gravity in the range 1.3-1.4. A bedrock basement was built in the flume using the bathymetry measured by Czapiga (2013), who conducted experiments under fully alluvial conditions using the crushed walnut shells. The supplemental material (S3) shows the bathymetry from those experiments. Transverse slopes were measured from ~~the point cloud~~the bathymetry, and a relation between transverse slope and streamwise location was fit to the data. Using it, transverse slopes every 0.5 m were calculated. Based on the computed transverse slopes, cross-sectional bathymetric slices were cut out of foam and placed inside the flume every 0.5 m. Pea gravel was used to fill the flume following the profile established by the foam slices. The region between streamwise stations CS07 and CS23 (Fig. 2c) was filled with gravel to an elevation slightly below the maximum given by the foam slices. This section was then covered with a ~ 1 cm layer of concrete and used to create the bedrock surface. We filled the rest of the flume (CS00 – CS07, and CS23 – CS30) with pea gravel to maintain an average centerline elevation throughout the flume. The size of the gravel was chosen so as to prevent it from being transported by the flow in the experiments. Figure 3c shows the bedrock bed built inside the Kinoshita Flume, and Fig. 2a shows its bathymetry. The concrete was painted white to enhance the contrast between the bedrock and the alluvium. The supplemental material (~~S1~~S1, S3) has a set of images and diagrams which provide additional information regarding the construction of the bedrock bed inside the flume and the pre-mixed concrete used.

The grain size distributions of the crushed walnut shells, the pea gravel, and the dry concrete mix (including gravel, sand and cement) are shown in Figure 3a. The inset figure includes the results of laser scans conducted to measure the as-built bedrock macro-roughness, i.e. the difference between the maximum and minimum elevations according to Zhang et al. (2015).~~.~~

2.3 Bed laser scans

A Keyence LB-1201 laser (Keyence, 1992) with sub-millimeter precision (250 µm) was used to scan the bed at five different locations, namely: CS10, CS12, CS15, CS17 and CS20 (Fig. 2c). These locations were chosen because they are representative of the bedrock topography at the apices (CS10, CS15 and CS20) and the crossings (CS12 and CS17). A polynomial was fit to the scans, and residual elevations were calculated by subtracting the actual reading from the polynomial. This removed the local topography from the signal. The average residual elevation along the cross sections was calculated and used to estimate the macro-roughness of the bedrock bed~~, i.e. the difference between the maximum and minimum elevations according to Zhang et al. (2015).~~ . The resulting value (10 mm) is also indicated in Fig. 3a. More details about the scans and the polynomial fit are included in the supplemental material (S1).

2.4 Areal alluvial cover measurements

The percentage of areal alluvial cover was calculated by analyzing time-lapse images of the flume bed. Images were taken, on average, every 10 s (0.1 Hz) during the duration of every run and processed in Matlab. A region of interest (ROI) was selected for each image series. In this study, the ROI corresponds to the middle bend of the Kinoshita flume, i.e. between streamwise locations 10 m and 20 m (Fig. 2).

Images were first converted to gray scale, and then the method of Otsu (1979), as implemented in Matlab ('graythresh' function), was used to make the images binary. The resulting black (alluvial cover) and white (bedrock) images were used to calculate the percent areal cover. The fraction of alluvial cover was determined as shown in Eq. 5.

(5)

In Eq. (5), percent of areal alluvial cover inside the region of interest; total number of pixels inside the region of interest (i.e. total area); and value of the j^{th} pixel in the binary image (white pixels are equal to one and black pixels are equal to zero). The pixel size in the images was approximately 2.8mm x 2.8mm. This resolution is not enough to capture individual sediment grains (D_{50} ~ 1.6 mm). Nevertheless, if a single grain lies in a pixel, ~ 25% of its area would be alluvium, leading to a gray pixel (as seen by MatLab). Depending on the threshold determined by Otsu's method for the region of interest, a single grain could be enough to be interpreted as alluvial cover. More details regarding the image acquisition and processing are included in the supplemental material (S2).

Formatted: Subscript

2.5 Relation between alluvial cover and sediment supply

A rectangular bedrock slab was built with the same materials used to build the bedrock basement in the flume. The bedrock slab was built over a piece of foam laid on a floor so as to have no longitudinal or transverse slope. Pea gravel was placed over the foam and a thin layer of concrete was poured over it. It was then painted white to increase contrast between the bedrock and the alluvium. The purpose of this bedrock slab, which was 0.6 m long by 0.4 m wide, was to measure i) the relation

between areal alluvial cover and sediment mass fraction, and ii) the relation between areal alluvial cover and the ratio of alluvial cover thickness to bedrock macro-roughness. Images of this simple experiment are included in the supplemental material (S1).

To quantify the cumulative sediment mass fraction, known weights of sediment were incrementally added to the slab and spread evenly until the bed was fully covered with alluvium. Eleven iterations were necessary to cover the bed completely. The total amount of mass used was 646 g. Mass increments used in every iteration are shown in supplement S1. The cumulative sediment mass fraction was calculated as the cumulative weight of sediment in every iteration, divided by the total weight of sediment used to fully cover the bed. Areal alluvial cover was quantified using images, and following the approach described in section 2.4. The ratio of alluvial cover thickness to bedrock macro-roughness was quantified by scanning nine cross sections of the bedrock slab with a sub-millimeter precision Keyence laser (Keyence, 1992). The cross sections were 4 cm away from each other. The first set of scans were conducted over the bare bedrock slab, and then they were repeated each time that alluvium was added over the slab. The entire process was conducted two times to verify that the results would not change due to any human-induced errors in the measurements or the way in which the alluvium was distributed over the bed after each iteration. After the first set of measurements, the alluvium was initially removed with a brush and then with an air-pressure hose to make sure no grains were left on the slab. Images related to this experiment are included in the supplemental material (S1).

2.6 Experimental conditions

Table 1 shows the general experimental conditions used in this study. The flow discharge rate used in all runs was 12.3 liters per second (Ls^{-1}) which corresponds to the flow rate used by Czapiga (2013). This flow rate created the alluvial bathymetry used to build the bedrock bed in theseis experiments. The flow discharge was measured with electromagnetic flow meters. Given that the sediment recirculating pump only works at a constant discharge of 3.1 Ls^{-1}, the main pump was set to have a discharge of 9.2 Ls^{-1}.

The volume of sediment inside the Kinoshita flume was modified between runs so as to obtain different reach-averaged areal ratios of alluvial cover. Runs in this study are identified based on this value (Table 2). For example, run "pc79" had 79% of the total bed area covered with alluvium after averaging in space (one wavelength) and time (one hour). The first run conducted was pc79.; Afer this run, we removed sediment from the flume, leading to lower pc conditions. The values obtained were not planned. fThe two following runs were ollowed by pc72 and pc54. Afterwards, all the sediment was removed from the system to run the bare-bedrock condition, pc00. The following runs were pc19, pc27, pc38 and pc46, conditions that were achieved after progressively adding sediment to the flume.

We allowed the bed to adjust for at least 8 hours between runs. The 60 minutes we report in the study are after the bed had adapted the new condition. We computed the alluvial cover statistics throughout the transition from one

state to another and once it had reached equilibrium we continued measuring. We report only the values once the system had reached equilibrium for each condition.

Formatted: English (United Kingdom)

Water surface slopes were initially calculated by using the water level elevation changes in the upstream and downstream tanks of the Kinoshita flume. Both tanks have a measuring tape glued to the upstream- and downstream-most walls (Fig. 2b). These measuring tapes were used to guarantee that runs always started at the desired water elevation. Before turning on the pumps, desired water elevations were verified, and after the run had started, readings were taken every 20-30 minutes.

Water surface elevations were also measured with eTapes in runs pc00, pc19, and pc79 (Fernández, 2018). An eTape is a sensor with a resistive output that varies with the level of fluid in which it is immersed. The resistive output of the sensor is inversely proportional to the height of the water. Low water depths correspond to high output resistance. Conversely, high water depths correspond to low output resistance. Details about the eTape installation, calibration, and operation are given in S4, and further information may be found in Fernández (2018). After runs pc79, pc72 and pc54 were finished, we noticed that the water surface slopes in the Kinoshita flume were different depending on if they were calculated for the total length of the flume, i.e. between tanks, or for the middle bend of the flume only. Figure 4 shows an example of the water surface elevations measured with the eTapes (middle zone of flume) and the measuring tapes (entire flume) for run pc79. To accurately measure the middle bend water surface slopes in runs pc00-pc46, point gages were placed on the flume at streamwise locations 9 m and 21 m (Fig. 2). The slopes calculated with the point gage readings are shown in Table 1. The average ratio of the slopes calculated with the point gages to those calculated with tank elevations in runs pc00 – pc46 was used to estimate the slopes in the middle bend of the flume for runs pc54, pc72 and pc79.

The sediment transport rates were measured by collecting material in ~~the~~ a ~~sediment trap~~box ~~located~~ fitted to the diffuser at the upstream end of the flume ~~.~~(Abad and Garcia, 2009b). This box is not shown in Figure 2. Table 2 shows the average sediment transport rates measured. ~~Average values are shown in Table 2.~~

2.6 Quantifying erosion potential

Based on Eq. 2, a dimensionless erosion potential E_{sp} may be expressed as a function of the areal fraction of alluvial cover as shown in Eq. 6 below. We use this (Sec. 3.5) to assess the spatio-temporal average erosion potential for the seven experimental conditions with alluvium.

(6)

At the microscopic level, the value of p_c can only take values of zero (exposed bedrock) or one (covered with alluvium). In the context of the areal images obtained during the experiments, this means that pixels may change between white and black throughout the run. This information may be used to quantify erosion potential based on alluvial cover fluctuations.

Bedrock incision can only occur when a particle strikes the bed. If a pixel changes from white to black between consecutive images, it means that sediment particles traveled into the area and struck the bed. If the pixel remains black or white in

consecutive images, no strikes occurred; and if the pixel changes from black to white, sediment particles have left, and thus did not strike the bed. With these definitions, the erosion potential may be quantified by counting the number of times that a pixel changes from white to black, i.e. by quantifying the fluctuations in alluvial cover.

The frequency of strikes (f_s) at the j^{th} pixel corresponds to the number of times that the j^{th} pixel has changed from white (p_c = 0) to black (p_c = 1) between consecutive images (im), divided by the total number of images (N) in the series (Eq. 7). We use this approach (Sec. 3.6) to assess the erosion potential based on alluvial cover fluctuations for the seven experimental runs containing alluvium.

(7)

3 Results

3.1 Relation between alluvial cover and sediment supply

Figure 5 shows the relation between alluvial cover and sediment supply measured on the bedrock slab and in the Kinoshita flume. Specifically, Figure 5a shows the relation between areal alluvial cover and cumulative sediment mass fraction measured on the bedrock slab. Figure 5b shows the relation between areal alluvial cover and the ratio of alluvial cover thickness to bedrock macro-roughness measured on the bedrock slab. The thin dashed lines with circle and square markers show the average results of the measurements; the thick dashed lines correspond to a best-fit line; and the dotted lines show the linear relation between variables that has been used by previous authors (e.g. Zhang et al., 2018, 2015; Inoue et al., 2016, 2014; Chatanatavet and Parker, 2009, 2008; Sklar and Dietrich, 2006, 2004). Figure 5c shows the relation between reach-averaged alluvial cover (spatial average measured over one wavelength) and sediment supply ratio measured in the Kinoshita flume.

~~Figure 6 shows a snapshot of the middle bend of the Kinoshita flume corresponding to each one of the eight reach-averaged alluvial cover conditions. Similar images for the bedrock slab experiment are included in the supplemental material (SX). Links to the videos showing the bed evolution for the different experimental conditions are included in the 'Video supplement' section at the end of the paper.~~

The relations between alluvial cover and sediment mass fraction in the bedrock slab (Fig. 5a) and the Kinoshita flume (Fig. 5c) are logarithmic (Eq. 8). The value of the constant 'a' in Eq. (8) below is different between the bedrock slab (a =0.23) and the Kinoshita flume (a = 0.14), but the shape of the relation is the same. Previous research has shown that ~~a linear~~different relations between ~~relation between~~ percent cover and sediment supply ratio ~~is~~ are valid under certain circumstances (e.g. Turowski and Hodge, 2017; Inoue et al, 2014; Chatanantavet and Parker, 2008) ~~but~~ and our results suggest that ~~a different~~the relation below is also possible:

(8)

This relation diverges as the sediment supply ratio (term in parentheses) tends towards zero and as such, does not describe the small sediment flux limit. The relation is similar to those derived by Turowski and Hodge (2017, Eqs. 27 and 31) when the exponential term in their relation is small. Aubert et al. (2016) predict a similar relation to describe the alluvial cover based on direct numerical simulations. In the case of the bedrock slab, the logarithmic relation suggests that, initially, the areal cover increases rapidly with sediment supply ratio. Once the smaller voids in the bed are filled, more and more alluvium is needed to fully cover the largest roughness elements and further increase p_c.

In the case of the Kinoshita flume, the logarithmic relation between alluvial cover and sediment supply ratio is believed to be due in large part to the formation of point bars and transient alluvial deposits. Initially, a small amount of alluvium covers a proportionately larger area of the bed, but as sediment supply increases, alluvial thickness growth is favored over areal extent of alluvial cover. As more alluvium accumulates over regions previously covered, additional sediment supplied to the reach tends to deposit at the edge of the existing deposits, thus increasing alluvial cover, but at an ever smaller rate.

Figure 5b shows the relation between areal alluvial cover and alluvial thickness to bedrock macro-roughness ratio. Zhang et al. (2018, 2015) and Inoue et al. (2014) used the assumption that the relation is linear but the results obtained for the bedrock slab suggest that an 'S-shaped' (sigmoid curve) relation is more appropriate. A logistic curve, which is a type of sigmoid curve, was fit to the measurements in this study. Eq. 9 shows the general logistic function and Eq. 10 shows the one used here. Comparing the two, it may be seen that: ; is the maximum value of the curve, corresponding to ; is the steepness of the curve; and is the x-value of the sigmoid curve's midpoint. As shown in Figure 5b and Eq. 10, the steepness used to fit the sigmoid curve to the measured values was 8 and the midpoint was defined at .

(9)

(10)

The function in Eq. 10 is valid between a characteristically low (e.g. 0.05) and a characteristically high (e.g. 0.95) value of to avoid unrealistic cover values (Zhang et al. 2018). It is likely that the steepness and midpoint value are associated with some measure of the grain size distribution of the alluvium and the macro-roughness height of the bedrock. In the case of the bedrock and alluvium (Fig. 3a) used in this study, the steepness value corresponds to and the mid-point value corresponds to . This issue merits further investigation so as to define appropriate relations to calculate the steepness and mid-point value of the sigmoid curve for implementation in numerical models. We discuss the issue of alluvial thickness and alluvial cover further in section 4.4.

~~(9)~~

~~(10)~~

Figure 6 shows a snapshot of the middle bend of the Kinoshita flume corresponding to each one of the eight reach-averaged alluvial cover conditions. Similar images for the bedrock slab experiment are included in the supplemental material (S1~~X~~). Links to the videos showing the bed evolution for the different experimental conditions are included in the 'Video supplement' section at the end of the paper.

3.2 Reach averages of alluvial cover fraction

Figure 7 shows the temporal evolution of reach-averaged alluvial cover for all experimental runs. Larger fractions of alluvial cover are associated with fluctuations about the mean value due to the appearance of freely-migrating bars as sediment supply increases. Figure 8 shows the maps of alluvial cover for all experimental runs. Darker shades of blue correspond to areas that were covered with alluvium for more than 70% of the time; and shades of yellow correspond to areas that were covered with alluvium less than 30% of the time. In regards to the 'tools' and 'cover' effects, the white and black regions in those alluvial cover maps would not experience erosion. No tools (alluvium) are available to erode the bed in the white regions whereas alluvium completely covered the bed in the black regions, thus protecting it from erosion.

The areal alluvial cover definition in Fig 1a is based on the assumption that alluvial deposits are transient, i.e. no portions of the bed in the reach remain persistently covered with alluvium or fully exposed. This assumption is not met in meandering channels where persistent alluvial cover deposits form and grow as sediment supply increases, and erosion may only occur in those regions where alluvial cover is changing in time, i.e. regions with transient cover.

3.3 Regions with transient alluvial cover

The alluvial cover maps in Figure 8 show different percentages of persistently covered or exposed bedrock, as well as regions with transient alluvial cover. The regions with transient alluvial deposits are those over which alluvial cover is changing in time (colored regions in Fig. 8). To delineate and quantify these areas, the following criteria were used: regions with persistent alluvial cover are those in which ; regions with persistent exposed bedrock are those in which ; and regions with transient alluvial cover are those in which . Using these criteria, maps of transient alluvial cover were prepared. Figure 9 shows the regions of transient cover (gray), persistent cover (black) and persistently exposed bedrock (white) for each of the eight experimental conditions. The area of the former two regions increases with sediment supply, whereas the area of the latter decreases as sediment supply increases.

Figure 10 shows the reach-averaged percentages of these three regions for all eight experimental conditions. Therein, the yellow dashed line corresponds to the reach-averaged fraction of persistently exposed bedrock; the blue line corresponds to the reach-averaged fraction of persistently covered bedrock; the light-blue line corresponds to the reach-averaged fraction of the bed with transient cover; the thick black line corresponds to the sum of the transient and persistent cover fractions; and the black dotted line corresponds to the 1:1 line.

The regions of persistent and transient cover increase as a function of reach-averaged alluvial cover. The regions of persistently exposed bedrock decrease concomitantly. In general, both the fraction of the total area with persistent and transient cover grow

at a similar rate with increasing reach-averaged p_c. The reach-averaged conditions for which transient and persistent cover have similar area ratios are p_c = 0.27, 0.46, 0.54 and 0.72. The largest differences between persistent and transient cover are observed at p_c = 0.19, 0.38 and 0.79.

The case p_c = 0.19 is likely due to the typical sedimentation patterns observed in meandering bedrock channels when alluvial point bars first form. Immediately downstream of the bend apices, i.e. points of highest curvature, sediment is deposited. In the Kinoshita flume, the apices of bends are located at streamwise locations 9.5 m, 14.5 m and 19.5 m (Fig. 13). Initially, these locations become the upstream-most points of the point bars. Once these deposits have been established, and as long as sediment continues to be supplied from upstream, the incoming particles travel above the existing deposit due to decreased resistance from the bed. Under such conditions, persistent alluvial cover is favored over transient alluvial cover.

The case p_c = 0.38 has a larger portion of the total area with transient cover than with persistent cover. As more sediment was supplied to the system while keeping the initial (no flow) water depth constant (Table 1), the alluvial thickness could not continue to grow indefinitely but rather, the areal extent of alluvial cover grew instead and the water-surface slope also increased (Table 2). Sediment particles could no longer be preferentially transported over the alluvial deposits, and began to be transported closer to the edge of the existing deposits.

The case p_c = 0.79 shows a dip in the ratio of transient cover, while the area with persistent cover continues to increase. Although there are no runs with a larger reach-averaged fraction of alluvial cover, it is likely that this trend would be maintained until the bed is completely covered with alluvium. As p_c grows, the area ratio of persistently covered regions should increase at a faster rate, and the area ratio of regions with transient cover should decrease rapidly towards zero. Eventually, the channel will not have any area left for the areal extent of alluvial cover to grow, so that further deposition promotes increased alluvial thickness instead. Erosion by abrasion would promote lateral migration of the bedrock river (e.g. Inoue et al., 2017; Shepherd, 1972).

~~The reach-averaged results shown in Fig. 8, Fig. 9 and Fig. 10 suggest that the areas subject to erosion in mixed bedrock-alluvial meandering rivers are a fraction of the total reach area. In the case of the Kinoshita flume experiments presented in this study, the areas with transient alluvial deposits occupied less than 50% of the total reach area, hence erosion could only occur within a restricted portion of total bed area.~~

3.4 Cross-section averages of alluvial cover

Figure 11 shows the cross-sectional alluvial cover averages for the seven experimental conditions with alluvium. Values were extracted every meter between streamwise locations 10 m and 20 m. Therefore, eleven local alluvial cover values were obtained for each experiment. As in the case of the reach-averaged values, these results include persistently covered and exposed portions of the cross section as well as a fraction with transient alluvial cover.

In general, all conditions exhibit similar trends, with local lows in p_c at streamwise locations 15 m and 19 m and local highs at streamwise locations 11 m and 16 m. The regions showing higher local percentages of alluvial cover are located 1.5 m downstream of the bend apices. Point bar deposits are responsible for the higher local value of p_c at these locations. On the

other hand, the local lows in p_c are associated with the points of highest curvature in the reach. Both local lows are within 0.5 m of the bend apices.

Figure 12 shows the ratios of the cross sections that had persistently exposed bedrock (dashed yellow line), persistently covered bedrock (blue line), transient alluvial cover (light-blue line), and the ratio corresponding to the sum of persistent plus transient cover (black line) for all experimental conditions but pc00. The ratio of exposed bedrock peaks in the vicinity of the bend apices. Even in the case of reach-averaged $p_c = 0.79$, portions of the bed in these areas remain exposed due to high curvature. Except for the cases with reach-averaged $p_c = 0.38$ and 0.54, no cross sections have fractions with transient alluvial cover greater than 60%.

The average fractions of transient alluvial cover at the cross-sectional level have values of 0.10 for $p_c = 0.19$, 0.21 for $p_c = 0.27$ and between 0.31 and 0.34 for the other experimental conditions. In spite of the local variations in transient alluvial cover, potential erosion is, on average, limited to a rather small portion of the cross section. This is likely due to the combined effects of sediment supply ratio and local curvature.

Figure 13 shows box plots of cross-sectionally averaged p_c normalized with the reach-averaged value. The figure also shows the dimensionless curvature of the Kinoshita flume (black dashed line), the negative value of the curvature (gray dotted line) and the median normalized values of p_c (red line). The true ( ) and negative ( ) centerline curvature signals are shown to better highlight the trend of normalized p_c with curvature.

The boxes include information from the seven experiments at each cross section. The median value is indicated by the red line inside the box; the bottom line on each box corresponds to the first quartile (q_1); the top line on each box corresponds to the third quartile (q_3); whiskers extend to $q_1 - 1.5(q_3 - q_1)$ at the bottom and $q_3 + 1.5(q_3 - q_1)$ at the top; and values lying outside this range are considered outliers and are indicated with a red cross. The cross sections located close to the bend apices, i.e. regions with local high curvature, show normalized p_c values below unity, whereas the regions with smaller curvature values show normalized p_c values above unity. Normalized, local p_c values follow the overall trend of local curvature.

3.5 Erosion potential based on alluvial cover averages

Figure 14 shows the erosion potential (Eq. 6) for all experimental conditions. Regions with higher erosion potential are those for which alluvial cover averages were close to 0.5, in accordance with the parabolic form of Eq. 6. These regions are shown in dark blue in figure 13. White regions have no erosion potential due to a lack of tools or the presence of alluvial cover protecting the bed from abrasion. The regions of potential erosion are limited to the areas with transient alluvial cover. In general, their width is a function of sediment supply ratio, with narrower regions associated with smaller sediment supply ratios. Locally, the width of these regions is affected by curvature as well, with narrower regions in areas of high curvature, and wider regions in areas of lower curvature.

The region of potential erosion is located closer to the inner bank for lower sediment supply ratios, and moves outward as sediment supply increases. Focusing on the region of potential erosion located at the bend apex at streamwise location 14.5 m

(see Fig. 2c for location on plots), it is seen that for $p_c = 0.27$, the region is located right next to the inside bank whereas for $p_c = 0.79$, the region is much closer to the outer bank. ~~Figure 15 shows an image of the mixed bedrock-alluvial Shimanto River in Shikoku, Japan and a sketch of what the cross section might look like with the areas of erosion and no erosion indicated. The reach shown in the image has an alluvial point bar on the inside of the bend, a narrow inset channel at the edge of the point bar and an exposed bedrock bench on the outside of the bend. The same morphologies have been observed in a smaller scale stream called Pescadero Creek, in California, USA (Fig. 6B in Johnson and Finnegan, 2015). The experiments of Mishra et al. (2018) also show that when sediment supply is low, the alluvial point bar is narrow and an inset channel is eroded at the toe of the point bar, leaving an exposed bedrock bench on the outer part of the bend.~~

~~The typical geometry of an alluvial meandering channel cross section is shallow on the inside and deep on the outside. The reach of the Shimanto River shown in Figure 15 has a different geometry. The deepest portion of the channel is not located on the outer bank. Instead, it is located at the toe of the point bar, which happens to be approximately at the middle of the cross section. It is likely that the narrow inset channel was formed during a long period of decreased sediment supply. During this period, the region of transient alluvial cover was confined to the current width of the channel shown in the image. The outer bedrock bench could potentially be eroded if sediment supplied to the reach from upstream were to be increased, and maintained at this increased value for an extended period of time. If this occurred, the point bar would likely extend toward the outer part of the bend, thus moving the area of transient alluvial cover farther into this region.~~

3.6 Erosion potential based on alluvial cover fluctuations

The results of alluvial cover shown and discussed up to this point correspond with spatial or temporal averages. Nonetheless, Fig. ~~16~~ 15 shows the frequency of strikes (f_s) for all experimental conditions (Eq. 7). In general, the areas in color in the figure are similar to the areas with transient alluvial cover shown in Fig. 9 and the areas with erosion potential in Fig. 14. Picking out differences in these particular figures is not straightforward, but the videos included in the supplemental material illustrate the migrating erosion fronts, and suggest that erosion is likely to be driven predominantly by the movement of freely-migrating bars. The use of the frequency of strikes associated with fluctuations in alluvial cover provides an improved approach for computing bedrock erosion by abrasion, as discussed below.

4 Discussion

4.1 Transient alluvial cover: An issue of timescales

Alluvial deposits on the bed of a bedrock river cover it and protect it from abrasion (Gilbert, 1877; Sklar and Dietrich, 1998; 2004). At the microscopic level, a portion of the river bed can only be covered ($p_c = 1$) or exposed ($p_c = 0$) in any given instant. Therefore, a notion of transient alluvial deposits becomes necessary to guarantee that in time, p_c fluctuates between those end members and erosion caused by saltating bedload particles is possible (Eq. 2). In the original saltation-abrasion framework of

Sklar and Dietrich (2004), transient alluvial deposits were an underlying assumption (Fig. 1a). No temporal averaging window was needed since all portions of the bed had the same probability of being eroded in time.

Turowski et al. (2007), working under the assumption that sediment transport capacity is uniform across a control area~~the width of a channel~~ of unspecified dimensions, described the cover effect as static or dynamic. Static cover occurs when the amount of sediment supplied to the reach is larger than the transport capacity, and therefore, some particles remain immobile on the bed. Dynamic cover occurs when the amount of sediment supplied is smaller than the transport capacity. Sediment particles cover portions of the bed but are mobile. As sediment supply increases, erosion is limited due to more grain-grain collisions than grain-bed interactions. In this framework, the dynamic cover effect reduces erosion by decreasing the impact energy experienced by the bed due to the interactions between grains. Nonetheless, the notion of transient alluvial cover over an unspecified time-window is required, and in the long term, all areas of the bed have the same likelihood of being eroded as long as sediment supply is below the transport capacity of the reach.

Chatanantavet and Parker (2008), Inoue et al. (2014), Hodge and Hoey (2016b), and Ferguson et al. (2017) present cases in which sediment particles are being transported over the bed as throughput bedload. These cases challenge the notion of a cover effect because alluvial deposits do not exist at all. They could still be treated as having transient alluvial cover for modeling purposes but what would be the relevant timescale to characterize it? Chatanantavet and Parker (2008), and Hodge and Hoey (2016b) also observed that throughput load may be unstable; as soon as hydraulic conditions change~~s~~, runaway alluviation occurred and the same portion of the bed changed from a state of being continuously struck by sediment particles (undergoing erosion) to being protected from further erosion.

The examples above~~,~~ suggest that areas with persistent or transient alluvial cover in a mixed bedrock-alluvial river can only be categorized as such given a specified timescale. The reach-averaged results shown in Fig. 8, Fig. 9 and Fig. 10 suggest that the areas subject to erosion in mixed bedrock-alluvial meandering rivers are a fraction of the total reach area. In this study, we defined transient alluvial cover as those portions of the bed where temporal averages of local alluvial cover had values between $0.025 < p_c < 0.975$ during the time of the experiment (Fig. 8). Based on this definition, areas with persistent alluvial cover or exposed bedrock were also delimited (Fig. 9). In the case of the Kinoshita flume experiments, the areas with transient alluvial deposits occupied less than 50% of the total reach area, hence erosion could only occur within a restricted portion of total bed area.

~~The reach-averaged results shown in Fig. 8, Fig. 9 and Fig. 10 suggest that the areas subject to erosion in mixed bedrock-alluvial meandering rivers are a fraction of the total reach area. In the case of the Kinoshita flume experiments presented in this study, the areas with transient alluvial deposits occupied less than 50% of the total reach area, hence erosion could only occur within a restricted portion of total bed area.~~

The problem remains in regards to generalizing appropriate timescales for modeling purposes. Our results are based on a constant discharge but in real rivers, a flood could mobilize all alluvium on the bed of the channel and within the timescale of the flood, alluvial cover would also be transient (e.g. Turowski and Rickenmann, 2009). The use of temporal averages of

alluvial cover has limitations, and our results suggest that characterizing the fluctuations of alluvial cover may be a better approach.

4.2 Alluvial cover fluctuations vs. averages

Figure ~~17~~ 16 shows a hypothetical example of two cases in which the long-term average of alluvial cover is equal, but the fluctuations in alluvial cover between them are different. Given that erosion by abrasion is driven by the number of times the bed is struck by particles, erosion would only occur in the first case. Erosion would only occur each time the area changes from white to black, i.e. every time a particle moves into the area and strikes the bed upon arrival. This simple example suggests that the use of temporal averages of alluvial cover to calculate erosion may lead to inaccurate results.

The use of a relation such as Eq. 2 with spatiotemporal averages of alluvial cover also has limitations. According to it, the following experiment pairs: i) $p_c = 0.19$ and $p_c = 0.79$; ii) $p_c = 0.27$ and $p_c = 0.72$; and iii) $p_c = 0.46$ and $p_c = 0.54$ should have very similar, or equal, erosion potentials (Eq. 6) as shown below:

i)

ii)

iii)

Figure 14 and the videos in the supplement show that the erosion potential in all cases is different, thus suggesting that spatial averaging may also lead to inaccurate results. For these reasons, temporal and spatial averages of alluvial cover are not appropriate to quantify erosion in mixed bedrock-alluvial rivers. The computational method of Inoue et al. (2016, 2017) both tracks the migration of cover fronts and bars and calculates cover at a spatiotemporally local level, thus approaching the methodology suggested here.

4.3 Regions of preferential erosion in mixed bedrock-alluvial meandering rivers

In spite of characterizing erosion potential with spatio-temporal averages (Fig. 14) or fluctuations (Fig. ~~16~~15) of alluvial cover, the regions of preferential erosion in our experiments show some characteristics that are worth discussing. In all experiments, the regions of preferential erosion are located at the edges of persistent alluvial cover deposits. Their precise location and width are a function of sediment supply and local curvature.

In general, as sediment supply increases, the areas of preferential erosion moved outwards. Our results suggest that in all cases, inset channels would have been formed at the edge of alluvial deposits and bank erosion would have only occurred beginning at CS11 (Fig. 2c, ~~16~~15) for pc54, pc72 and pc79. Downstream of CS15, outer bank erosion would only occur for the cases with pc72 and pc79. Therefore, higher sediment supply is needed for bank erosion to occur, and under low sediment supply, inset channels and outer bedrock benches, ~~e.g. of the type observed on the Shimanto River,~~ are likely to form. ~~(Fig. 15).~~

Figure 157 shows an image of the mixed bedrock-alluvial Shimanto River in Shikoku, Japan and a sketch of what the cross section might look like with the areas of erosion and no erosion indicated. The reach shown in the image has an alluvial point bar on the inside of the bend, a narrow inset channel at the edge of the point bar and an exposed bedrock bench on the outside of the bend. The same morphologies have been observed in a smaller scale stream called Pescadero Creek, in California, USA (Fig. 6B in Johnson and Finnegan, 2015). The experiments of Mishra et al. (2018) also show that when sediment supply is low, the alluvial point bar is narrow and an inset channel is eroded at the toe of the point bar, leaving an exposed bedrock bench on the outer part of the bend.

The typical geometry of an alluvial meandering channel cross section is shallow on the inside and deep on the outside. The reach of the Shimanto River shown in Figure 157 has a different geometry. The deepest portion of the channel is not located on the outer bank. Instead, it is located at the toe of the point bar, which happens to be approximately at the middle of the cross section. It is likely that the narrow inset channel was formed during a long period of decreased sediment supply. During this period, the region of transient alluvial cover was confined to the current width of the channel shown in the image. The outer bedrock bench could potentially be eroded if sediment supplied to the reach from upstream were to be increased, and maintained at this increased value for an extended period of time. If this occurred, the point bar would likely extend toward the outer part of the bend, thus moving the area of transient alluvial cover farther into this region.

~~Therefore, higher sediment supply is needed for bank erosion to occur, and under low sediment supply, inset channels and outer bedrock benches, e.g. of the type observed on the Shimanto River, are likely to form (Fig. 15).~~

Finnegan et al. (2007) observed similar trends in experiments conducted in a straight flume over an erodible bed, where erosion began at the edges of sediment patches and formed longitudinal grooves in the channel. Shepherd and Schumm (1974) also observed that outward bank erosion was possible when bed material was transported at capacity, but when the amount of material in transport was less than the transport capacity, inset channels formed. Similar observations have been made experimentally by Mishra et al. (2018) and numerically by Inoue et al. (2017), and Nelson and Seminara (2011). Even though we did not measure velocities, our observations suggest that the areas with very narrow regions of erosion potential, e.g. between CS14 and CS15, are located at regions of topographically induced high flow velocities in accordance with observations made by Hodge and Hoey (2016b).

The specific links between sediment supply and local curvature, even though suggested by our results, need further investigation to properly parameterize them. It is likely that antecedent curvature and curvature sign also play a role (Fig. 13). Moreover, the use of denser material, e.g. sand, would likely affect the specific locations of the alluvial deposits. However, the main trends observed herein are likely to be general.

4.4 Alluvial thickness and alluvial cover

The results corresponding to the Kinoshita flume are based on areal cover of alluvial sediment captured with a camera located above the flume. These observations are related to the framework of Sklar and Dietrich (2004) described in Fig. 1a. The framework proposed by Zhang et al. (2018, 2015) and shown in Fig. 2b, relates to the experiment conducted in the small

bedrock slab (S~~X~~1, Fig. 5) where the cover is quantified as in Eq. 4. That experiment allowed us to relate the areal cover fraction to the ratio of alluvial thickness to bedrock macro-roughness (Fig. 5b). We obtained and S-shaped relation between these two variables.

This result provides a useful link between the two models (Fig. 1a and 1b) but is only constrained by geometric variables, specifically the alluvium grain size and the bedrock macro-roughness. Other factors that affect the distribution and size of alluvial deposits are: local topography and hydraulic conditions (e.g. Hodge and Hoey, 2016b; Chatanantavet and Parker, 2008; Finnegan et al., 2007; Johnson and Whipple, 2007), grain size and ratio between grain and bedrock roughness (e.g. Ferguson et al., 2017; Nelson et al. 2014; Johnson 2014; Inoue et al. 2014; Chatanantavet and Parker, 2008), feedbacks between bedrock erosion, sediment deposition and its effects on hydraulic resistance (e.g. Ferguson et al. 2017; Nelson et al. 2014; Jonhson, 2014; Inoue et al. 2014) and channel sinuosity (Shepherd and Schumm 1974; Shepherd, 1972).

The relations between amount of sediment in the system and alluvial cover in Fig. 5a and Fig. 5c are similar but are not equivalent. Figure 5a is based on the cumulative mass of sediment added to the bedrock slab, whereas Fig. 5c is based on the sediment supply ratio (Eq. 3). Turowski and Hodge (2017) developed an equation to relate the sediment mass on the bed and sediment supply. Their model differentiates between the mass of mobile and stationary bed material and relates them to sediment flux via an entrainment-deposition equation. Their framework could be tested with our dataset. Two particular issues of interest are:

i) The area of exposed bedrock is a function of the sediment mass in the system and the probability of incoming particles striking open bed areas. Turowski and Bloem (2015) showed that ~~erosion is possible~~particle impact energy can be transferred to the bed if the thickness of the alluvial layer, even if static, is small. However, they concluded that the amount of energy transferred to the bed is negligible in comparison to those areas where a sediment particle impacts the bed directly; in the long term direct impacts are likely to dominate bed erosion. Therefore, parameterizing these open areas is very important to better model bedrock erosion. Our results show that different areas of the bed have different likelihoods of being eroded. Our dataset could be used to develop a probability function that takes into account the effects of local curvature.

ii) In the model of Turowski and Hodge (2017), steady state cover is controlled by a characteristic dimensionless mass of sediment, which is equal to the ratio between dimensionless transport capacity and particle speed. This mass is converted to dimensional variables with the help of a characteristic mass, defined by the authors as the minimum mass of sediment required to completely cover the bed per unit area. This minimum mass is likely to be dependent on the ratio between grain size and bedrock macro-roughness.

Generally speaking, two scenarios are possible: If the grain roughness is larger than the bedrock macro-roughness, the minimum mass of sediment can be determined as proposed by the authors (~~Hodge and Hoey~~Turowski and Hodge, 2017; Eq. 34); If the bedrock macro-roughness is larger than the grain roughness, the equation could be adapted by multiplying it by, e.g. D_{84}/L_{mr}, to account for the fact that more grains are needed to fill the holes in the bedrock surface. The ratio suggested is based on the value obtained for the sigmoid function

relating areal cover and alluvial thickness in the bedrock slab (Eq. 10). The specific grain size chosen and the definition of the macro-roughness length are issues that need further investigation. The latter issue in particular is still unresolved in the bedrock river literature, where some authors characterize macro-roughness as the standard deviation of the bed elevation signal (e.g. Hodge and Hoey, 2016a, b), but others, such as us, use a characteristic length based on the bed hypsometry (e.g. Zhang et al. 2018, 2015).

5 Conclusions

The results of this study lead to the following conclusions:

1. The percent of areal alluvial cover initially grows rapidly with increasing sediment supply ratio in meandering channels. Rapid initial growth is likely due to the formation of point bars. Following the formation of these initial deposits, addition of more sediment into the system first promotes the growth of alluvial thickness, and later promotes the growth of the areal extent of alluvial cover. Therefore, a logarithmic relation between these variables reflects their relation better than a linear one. A logarithmic relation allows for rapid initial growth of p_c with increasing sediment supply ratio, but as the sediment supply ratio increases, growth in p_c slows down.
2. The percent areal alluvial cover as a function of the ratio between alluvial thickness and bedrock macro-roughness follows an S-shaped (sigmoid) curve. A logistic curve is recommended for models of bedrock erosion that use this framework.
3. The steepness and intersection parameters needed in the logistic curve are likely functions of a characteristic grain size of the alluvium and the bedrock macro-roughness. In this study, the steepness and intersection values used were given by and respectively.
4. Mixed bedrock-alluvial meandering channels may have areas with persistent and transient alluvial cover as well as areas of persistently exposed bedrock. Erosion by abrasion is possible only in the areas with transient alluvial cover. Local normalized p_c values are smaller than reach-averaged values at regions with high curvature and higher at regions with lower curvature.
5. The size and location of the areas of preferential erosion in mixed bedrock-alluvial meandering rivers are a function of sediment supply ratio and local curvature. Low sediment supply ratios are associated with regions of potential erosion located closer to the inner bank. This region moves toward the outer bank as sediment supply increases. High local curvature values are associated with narrow regions of potential erosion whereas lower curvature values are associated with wider regions of potential erosion.
6. The use of either spatially or temporally averaged values of p_c, or a combination of both, is not necessarily an appropriate approach to model bedrock erosion by abrasion of bedload. The largest spatial window recommended should be as small as possible so as to capture the local spatiotemporal fluctuations in alluvial cover. The longest

temporal window recommended should be quasi-instantaneous so as to capture the temporal fluctuations in alluvial cover.

5.1 Future research directions

Based on the results of this study, the following two research directions are proposed:

1. Conduct experiments with the objective of determining appropriate relations to define the steepness and intersection of the sigmoid function for use in numerical models of bedrock erosion based on a framework using ratio of alluvial thickness to bedrock macro-roughness.
2. Develop a model of bedrock erosion by abrasion based on the fluctuations of areal alluvial cover. The model must take into consideration the role of freely-migrating bars and their celerity. The numerical formulation of Inoue et al. (2017, 2016) offers an important advance in this regard.

Code Availability

The Matlab routines developed to process the time lapse images and eTape data are available at https://doi.org/10.13012/B2-3044828_V1.

Data availability

All data used in preparation of this manuscript is available at https://doi.org/10.13012/B2-3044828_V1.

Video supplement

Videos showing the evolution of the bed and the erosion fronts are available at:
https://av.tib.eu/series/606/experiments+on+patterns+of+alluvial+cover+and+bedrock+erosion+in+a+meandering+channel

Author contributions

Experiments were designed by all authors. R. Fernández conducted the experiments, data analysis and post-processing. Initial manuscript was prepared by R. Fernandez and G. Parker. All authors worked on the final version submitted.

Competing interests

The authors declare that they have no conflict of interest.

Acknowledgements

We would like to thank the Associate Editor Eric Lajeunesse for his patience and feedback during the open discussion and review process. We would also like to thank Jens Turowski and Christian Braudrick for their constructive reviews and very valuable feedback. Participation of all authors in this study was possible thanks to funding provided by the US National Science Foundation [grant EAR1124482]. The authors would like to thank Alejandro Vitale, PhD for his help building the eTape system, assistance with Arduino code development, and preparation of the wiring diagram.

References

Abad, J. D., and Garcia, M.H.: Experiments in a high-amplitude Kinoshita meandering channel: 1. Implications of bend orientation on mean and turbulent flow structure, Water Resour. Res., 45, W02401, https://doi.org/10.1029/2008WR007016, 2009a.

Abad, J. D., and Garcia, M.H.: Experiments in a high-amplitude Kinoshita meandering channel: 2. Implications of bend orientation on bed morphodynamics, Water Resour. Res., 45, W02402, https://doi.org/10.1029/2008WR007017, 2009b.

Beer, A. R., and Turowski, J. M.: Bedload transport controls bedrock erosion under sediment-starved conditions. Earth Surf. Dynam., 3, 291–309, 2016 https://doi.org/10.5194/esurf-3-291-2015, 2015.

Beer, A. R., Kirchner, J.W., and Turowski, J.M.: Graffiti for science – erosion painting reveals spatially variable erosivity of sediment-laden flows. Earth Surf. Dynam., 4, 885–894, 2016 https://doi.org/10.5194/esurf-4-885-2016, 2016.

Beer, A. R., Turowski, J.M., and Kirchner, J.W.: Spatial patterns of erosion in a bedrock gorge, J. Geophys Res-Earth, 122, 191–214, https://doi.org/10.1002/2016JF003850, 2017.

Chatanantavet, P., and Parker, G.: Physically based modeling of bedrock incision by abrasion, plucking, and macroabrasion, J. Geophys. Res., 114, F04018, https://doi.org/10.1029/2008JF001044, 2009

Chatanantavet, P., and Parker, G.: Experimental study of bedrock channel alluviation under varied sediment supply and hydraulic conditions, Water Resour. Res., 44, W12,446, https://doi.org/10.1029/2007WR006581, 2008

Cook, K.L, Turowski, J.M., and Hovius, N.: A demonstration of the importance of bedload transport for fluvial bedrock erosion and knickpoint propagation. Earth Surf. Proc. Land., 38, 683-695, https://doi.org/10.1002/esp.3313, 2013.

Cook, K.L., Whipple, K.X, Heimsath, A.M., and Hanks, T.C.: Rapid incision of the Colorado River in Glen Canyon – insights from channel profiles, local incision rates, and modelling of lithologic controls. Earth Surf. Proc. Land., https://doi.org/10.1002/esp.1790, 2009.

Czapiga, M.: Systematic Connectivity in Single Thread Meandering Alluvial Rivers: Statistical Generalization of Hydraulic Geometry. MSc thesis, University of Illinois at Urbana-Champaign, http://hdl.handle.net/2142/44498, 2009.

Ferguson, R.I., Sharma, B.P., Hodge, R.A., Hardy, R.J., and Warburton, J.: Bed load tracer mobility in a mixed bedrock/alluvial channel. J. Geophys. Res.-Earth, 122, 807-822, https://doi.org10.1002/2016JF003946, 2017.

Fernández, R.: Laboratory experiments on alluvial cover in mixed bedrock-alluvial meandering channels and on the formation and evolution of supraglacial meltwater meandering streams. PhD Thesis. University of Illinois at Urbana-Champaign. http://hdl.handle.net/2142/101494, 2018.

Fernández, R., Parker, G., and Stark, C.: Experiments on patterns of alluvial cover and bedrock erosion in a meandering channel. University of Illinois at Urbana-Champaign. https://doi.org/10.13012/B2-3044828_V1, 2019.

Finnegan, N. J., Sklar, L. S., and Fuller, T. K.: Interplay of sediment supply, river incision, and channel morphology revealed by the transient evolution of an experimental bedrock channel. J. Geophys. Res.-Earth, 112(3):1–17, https://doi.org/10.1029/2006JF000569, 2007.

Gasparini, N. M., Whipple, K. X., and Bras, R. L.: Predictions of steady state and transient landscape morphology using sediment-flux-dependent river incision models. J. Geophys. Res.-Earth, 112(3):1–20, https://doi.org/10.1029/2006JF000567, 2007

Gilbert, G.: Geology of the Henry Mountains. Technical report, U.S. Department of the Interior, 1877.

Hodge, R., and Hoey, T.B.: A Froude-scaled model of a bedrock-alluvial channel reach: 2. Sediment cover. J. Geophys. Res.-Earth, 121, 1597-1618, https://doi.org10.1002/2015JF003709, 2016.

Hodge, R., Hoey, T., Maniatis, T., and Lepretre, E.: Formation and erosion of sediment cover in an experimental bedrock-alluvial channel. Earth Surf. Proc. Land., 41, 1409-1420, https://doi.org/10.1002/esp.3924, 2016

Hodge, R., Hoey, T.B., and Sklar, L.: Bed load transport in bedrock rivers: The role of sediment cover in grain entrainment, translation, and deposition. J. Geophys. Res., 116, F04028, https://doi.org/10.1029/2011JF002032, 2011.

Inoue, T., Parker, G., and Stark. C.P.: Morphodynamics of a bedrock-alluvial meander bend that incises as it migrates outward: Approximate solution of permanent form. Earth Surf. Proc. Land., 42, 1342-1354, https://doi.org/10.1002/esp.4094, 2017.

Inoue, T., Iwasaki, T., Parker, G., Shimizu, Y., Izumi, N., Stark, C.P. and Funaki, J.: Numerical simulation of effects of sediment supply on bedrock channel morphology. J. Hydraul. Eng., 142(7), 04016014, https://doi.org /10.1061/(ASCE)HY.1943-7900.0001124, 2016.

Inoue, T., Izumi, N., Shimizu, Y., and Parker, G.: Interactions among alluvial cover, bed roughness, and incision rate in purely bedrock and alluvial-bedrock channel. J. Geophys. Res.-Earth, 119, 2123–2146 https://doi.org/10.1002/2014JF003133, 2014.

Johnson, J.P.: A surface roughness model for predicting alluvial cover and bed load transport rate in bedrock channels. J. Geophys. Res.-Earth, 119, 2147-2173, https://doi.org/10.1002/2013JF003000, 2014

Johnson, J. P., and Whipple, K.X.: Evaluating the controls of shear stress, sediment supply, alluvial cover, and channel morphology on experimental bedrock incision rate, J. Geophys. Res., 115, F02018, https://doi.org 10.1029/2009JF001335, 2010.

Johnson, J. P., and Whipple, K.X.: Feedbacks between erosion and sediment transport in experimental bedrock channels, Earth Surf. Proc. Land., 32, 1048–1062, https://doi.org/10.1002/esp.1471, 2007.

Johnson, K.N., and Finnegan, N. J.: A lithologic control on active meandering in bedrock channels. Geol. Soc. Am. Bull., 127(11/12), 1766-1776, https://doi.org/10.1130/B31184.1, 2015.

Keyence Corporation. Laser Displacement Sensors, Instruction Manual, LB-1000(W) Series. Japan. 24pp, 1992.

Lague, D.: Reduction of Long-Term Bedrock Incision Efficiency by Short-Term Alluvial Cover Intermittency. J. Geophys. Res.-Earth, 115, F2, F02011, https://doi.org/10.1029/2008JF001210, 2010.

Lamb, M. P., Dietrich, W.E., and Sklar, L.S.: A model for fluvial bedrock incision by impacting suspended and bedload sediment, J. Geophys. Res., 113, F03025, https://doi.org/10.1029/2007JF000915, 2008

Mishra, J., Inoue, T., Shimizu, Y., Sumner, T., and Nelson, J.M.: Consequences of abrading bed load on vertical and lateral erosion in a curved experimental channel. J. Geophys. Res.-Earth, 123, 3147-3161, https://doi.org/10.1029/2017JF004387, 2018.

Nelson, P.A., Bolla Pittaluga, M., and Seminara, G.: Finite amplitude bars in mixed bedrock-alluvial channels. J. Geophys. Res.-Earth. 119, 566-587, https://doi.org/10.1002/2013JF002957, 2014.

Nelson, P.A., and Seminara, G.: A theoretical framework for the morphodynamics of bedrock channels. Geophys. Res. Lett., 39, L06408, https://doi.org/10.1029/2011GL050806, 2012.

Nelson, P.A., and Seminara, G.: Modeling the evolution of bedrock channel shape with erosion from saltating bedload. Geophys. Res. Lett., 38, L17406, doi:10.1029/2011GL048628, 2011.

Otsu, N.: A Threshold Selection Method from Gray-Level Histograms. IEEE T. Sys. Man Cyb., 9(1), 62-66, 1979.

Shepherd (1972)

Shepherd and Schumm (1974)

Sklar, L. S., and Dietrich, W. E.: The role of sediment in controlling steady-state bedrock channel slope: Implications of the saltation abrasion incision model. Geomorphology, 82, 58–83, https://doi.org/10.1016/j.geomorph.2005.08.019, 2006.

Sklar, L. S., and Dietrich, W.E.: A mechanistic model for river incision into bedrock by saltating bedload, Water Resour. Res., 40, W06301, https://doi.org/10.1029/2003WR002496, 2004.

Sklar, L. S., and Dietrich, W. E.: Sediment and rock strength controls on river incision into bedrock. Geology, 29(12), 1087-1090, https://doi.org/10.1130/0091-7613(2001)029<1087:SARSCO>2.0.CO;2, 2001.

Sklar, L.S., and Dietrich, W.E.: River longitudinal profiles and bedrock incision models: stream power and the influence of sediment supply. Rivers over rock: Fluvial processes in bedrock channels. Geophysical Monograph 107. American Geophysical Union, https://doi.org/10.1029/GM107p0237, 1998.

Turowski, J.M.: Alluvial cover controlling the width, slope and sinuosity of bedrock channels. Earth Surf. Dynam. 6:29-48, https://doi.org/10.5194/esurf-6-29-2018, 2018.

Turowski, J.M., and Bloem (2015)

Turowski, J.M., and Hodge, R.: A probabilistic framework for the cover effect in bedrock erosion. Earth Surf. Dynam., 5, 311–330, https://doi.org/10.5194/esurf-5-311-2017, 2017.

Turowski, J. M., Hovius, N., Meng-Long, H., Lague, D., and Men-Chiang, C.: Distribution of erosion across bedrock channels. Earth Surf. Proc. Land., 33:353–363, https://doi.org/10.1002/esp.1559, 2008.

Turowski, J. M., Lague, D., and Hovius, N.: Cover effect in bedrock abrasion: A new derivation and its implications for the modeling of bedrock channel morphology. J. Geophys. Res., 112, F04006, https://doi.org/10.1029/2006JF000697, 2007.

Turowski, J.M., and Rickenmann, D. (2009)

Whipple, K. X., Hancock, G. S., and Anderson, R. S.: River incision into bedrock: Mechanics and relative efficacy of plucking, abrasion, and cavitation. Geol. Soc. Am. Bull., 112(3), 490–503, https://doi.org/ 10.1130/0016-7606(2000)112<490:RIIBMA>2.0.CO, 2000.

Zhang, L., Stark, C., Schumer, R., Kwang, J., Li, T., Fu, X., et al.: The advective-diffusive morphodynamics of mixed bedrock-alluvial rivers subjected to spatiotemporally varying sediment supply. J. Geophys. Res.-Earth, 123, 1731-1755, https://doi.org/10.1029/2017JF004431, 2018.

Zhang, L., Parker, G., Stark, C. P., Inoue, T., Viparelli, E., Fu, X., and Izumi, N.: Macro-roughness model of bedrock alluvial river morphodynamics. Earth Surf. Dynam., 3, 113–138, https://doi.org/10.5194/esurf-3-113-2015 , 2015.

Table 1 Hydraulic parameters common to all experimental conditions

Parameter		Value
Flow discharge	Q [m^3/s]	0.0123
Channel width	B [m]	0.60
Centerline depth	H [m]	0.11
Reach-averaged velocity	U [m/s]	0.19
Hydraulic radius	R_h [m]	0.08
Froude number	F_r [-]	0.18

Table 2 Experiment parameters specific to each run.

Run ID	Reach-averaged fraction of cover	Water Temperature	Average bed load transport rate	Water surface slope, middle bend	Water surface slope, entire flume	Kinematic viscosity	Reynolds Number
[-]	p_c [-]	T [°C]	q_{bs} [g/s]	S [mm/m]	S [mm/m]	[mm^2/s]	R_e [-]
pc00	0.00	24	0.00	0.99	0.68	0.9131	16,328
pc19	0.19	20	0.08	0.97	0.79	1.0034	14,859
pc27	0.27	24	0.25	0.99	0.75	0.9131	16,328
pc38	0.38	27	0.55	1.14	0.88	0.8539	17,460
pc46	0.46	21	1.47	1.19	1.01	0.9795	15,221
pc54	0.54	22	- [a]	1.0~~3~~ [b]	0.79	0.9565	15,587
pc72	0.72	27	4.50	1.3~~26~~ [b]	0.97	0.8539	17,460
pc79	0.79	24	5.60	1.3~~26~~ [b]	0.97	0.9131	16,328

[a] Bed load transport rate not measured for this condition.

[b] Slopes estimated based on the average ratio between middle bend slopes to flume slopes of previous five experimental conditions.

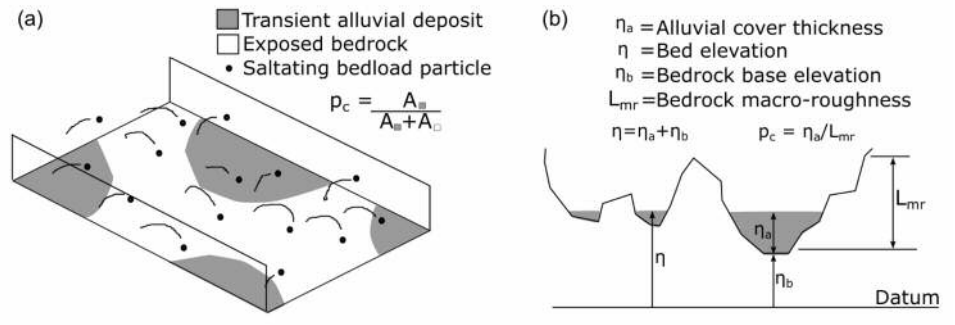

Figure 1. Schematic representations of (a) the fraction of exposed bedrock showing surface areal cover (Sklar and Dietrich, 2004) and (b) a cross section illustrating filling of a rough bedrock surface with alluvium (Zhang et al., 2015).

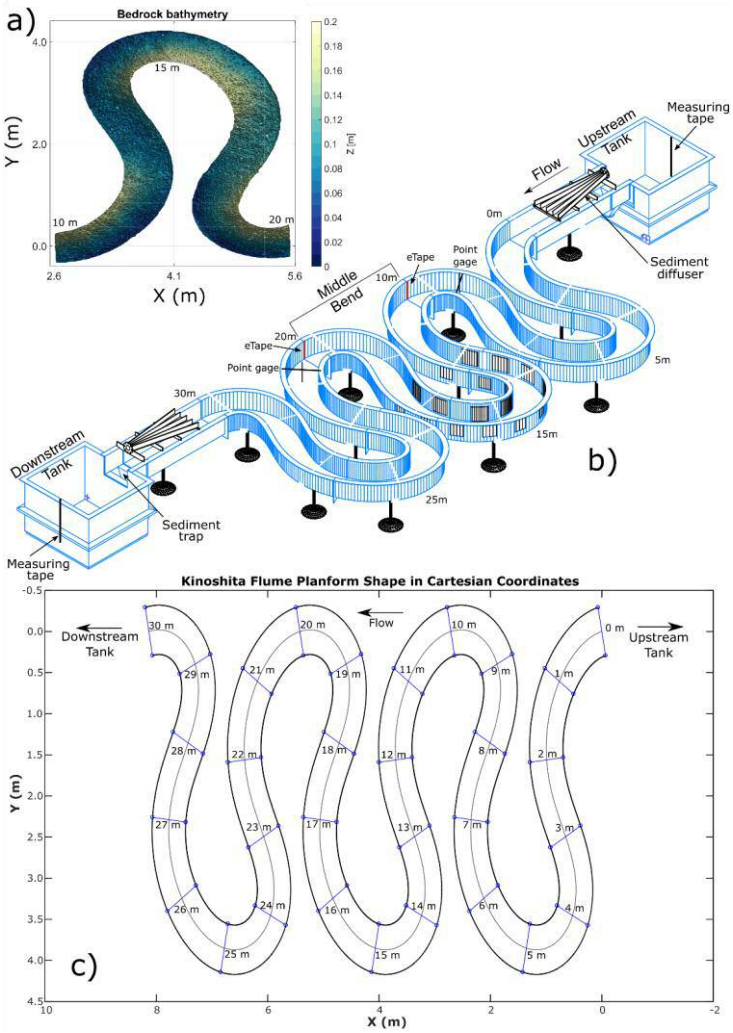

Figure 2: a) Bedrock bathymetry built inside the Kinoshita flume. Streamwise locations 10m, 15m and 20m are indicated; b) 3D rendering of Kinoshita flume showing location of tank measuring tapes, point gages, eTapes, sediment trap and sediment diffuser, flow direction, and middle bend where all measurements were made; c) Kinoshita shape with streamwise stations indicated. Flow direction from right to left.

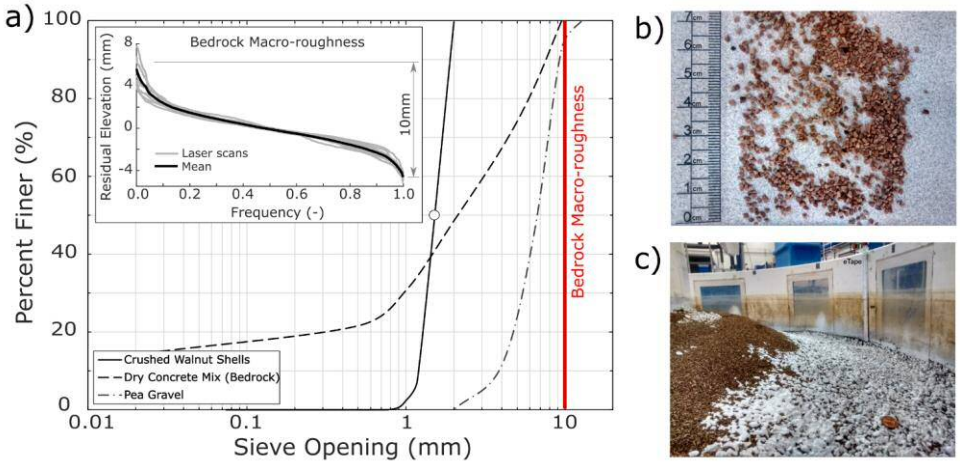

Figure 3. a) Grain size distributions for the alluvium (crushed walnut shells), dry concrete mix used to build the bedrock, and the pea gravel underlying the bedrock basement. Insert shows residual elevations of as-built bedrock bed, measured with laser scans at different cross sections inside the Kinoshita flume. Mean macro-roughness (~10mm) is also indicated in the main plot; b) Image of crushed walnut shells with ruler for scale; and c) Bedrock bed partially covered with alluvium inside the Kinoshita flume.

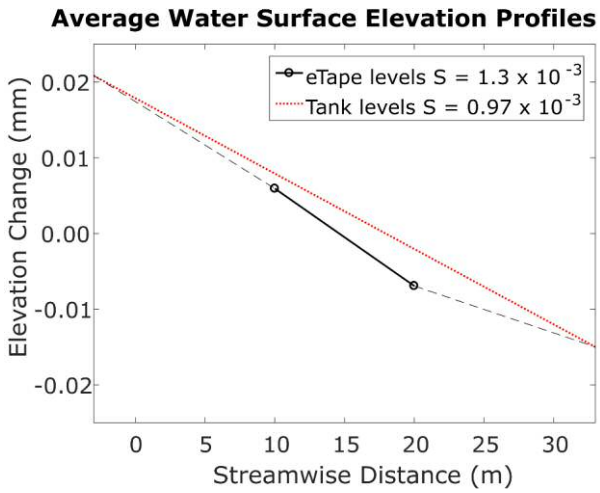

Figure 4 Average water surface elevation profiles and corresponding slopes based on the eTape readings and the levels measured in the upstream and downstream tanks for Run pc79.

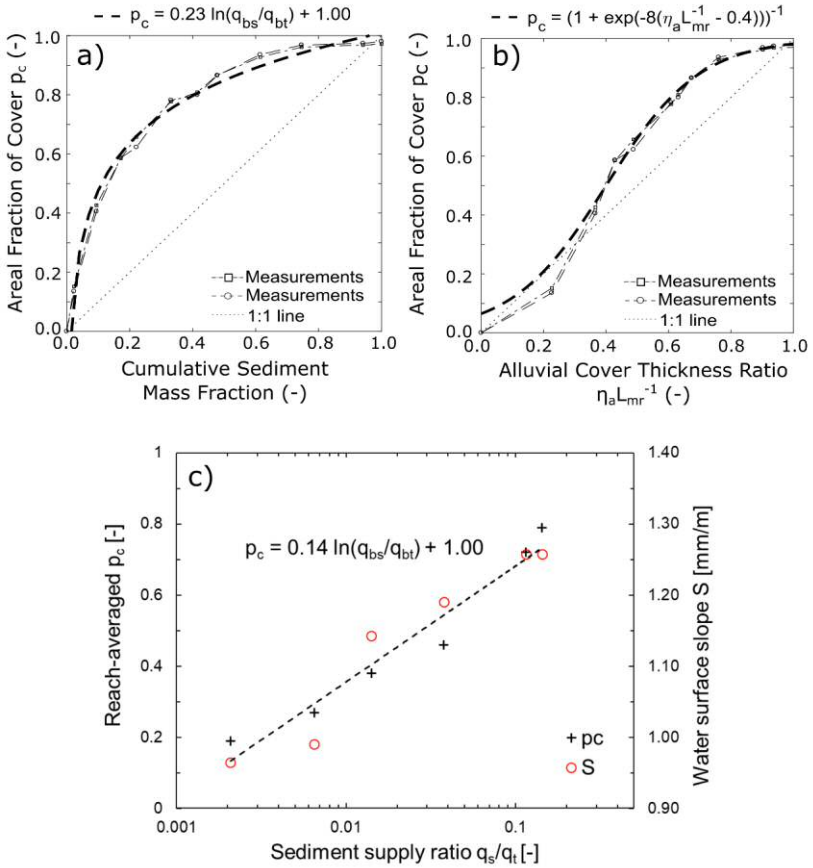

Figure 5 a) Relation between areal fraction of alluvial cover and cumulative sediment mass fraction for bedrock slab, total mass added to the slab was 646 g and all increments are shown in supplement S1; b) Relation between areal fraction of alluvial cover and the ratio between alluvial thickness and bedrock macro-roughness for bedrock slab; c) Relation between reach-averaged areal fraction of alluvial cover and sediment supply ratio for Kinoshita flume and corresponding water surface slopes as a function of sediment supply ratio.

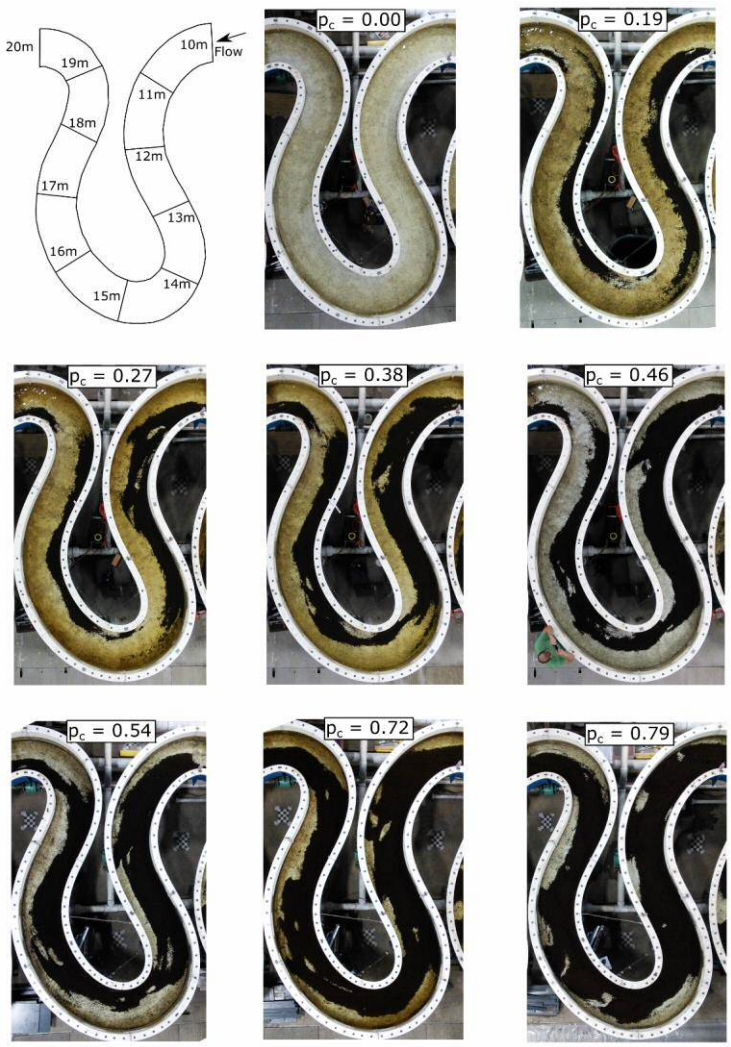

Figure 6 Images of the middle bend of the Kinoshita flume corresponding to an instant during each of the eight different areal alluvial cover conditions. Volume of sediment in the system grows from top to bottom and left to right. Diagram included at the top-left shows flow direction and contains cross sections indicating the streamwise locations along the middle bend of the flume.

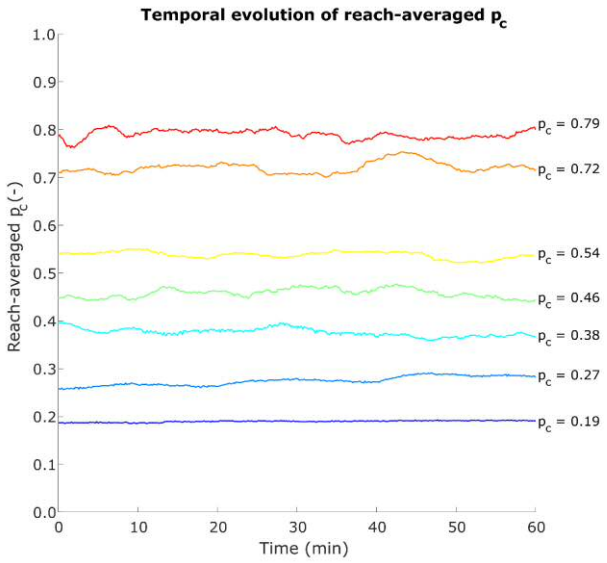

Figure 7 Temporal evolution of reach-averaged areal fraction of alluvial cover for all experimental conditions that had alluvium.

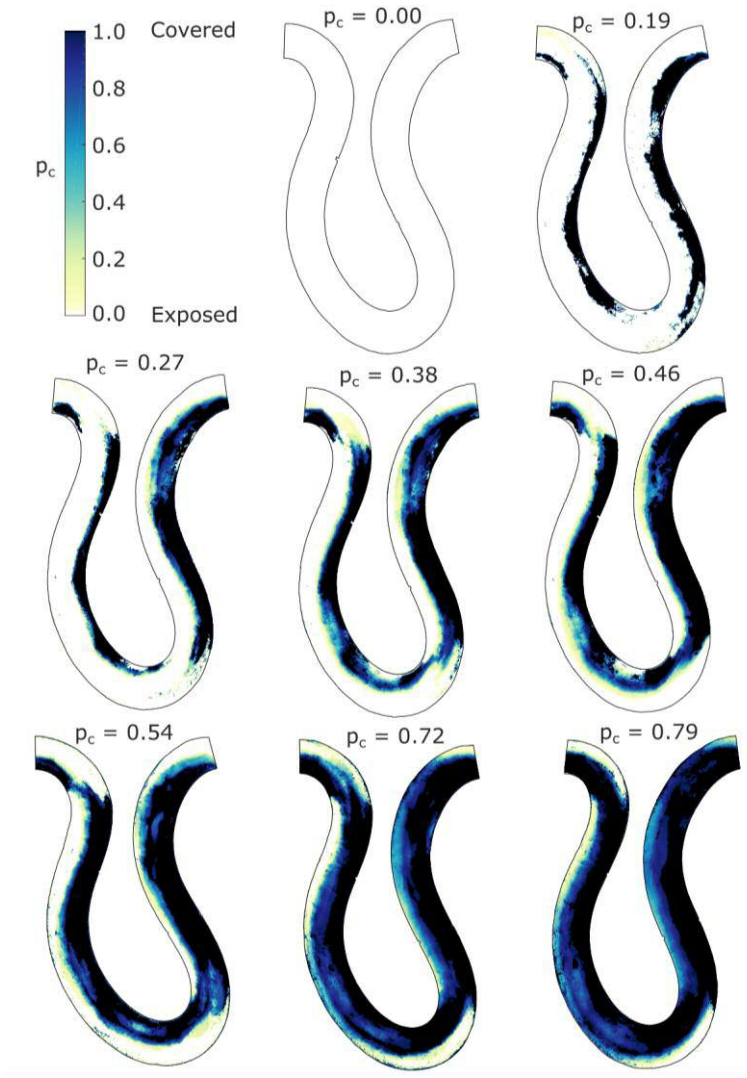

Figure 8 Maps of spatiotemporal averages of areal fraction of alluvial cover for all experimental conditions.

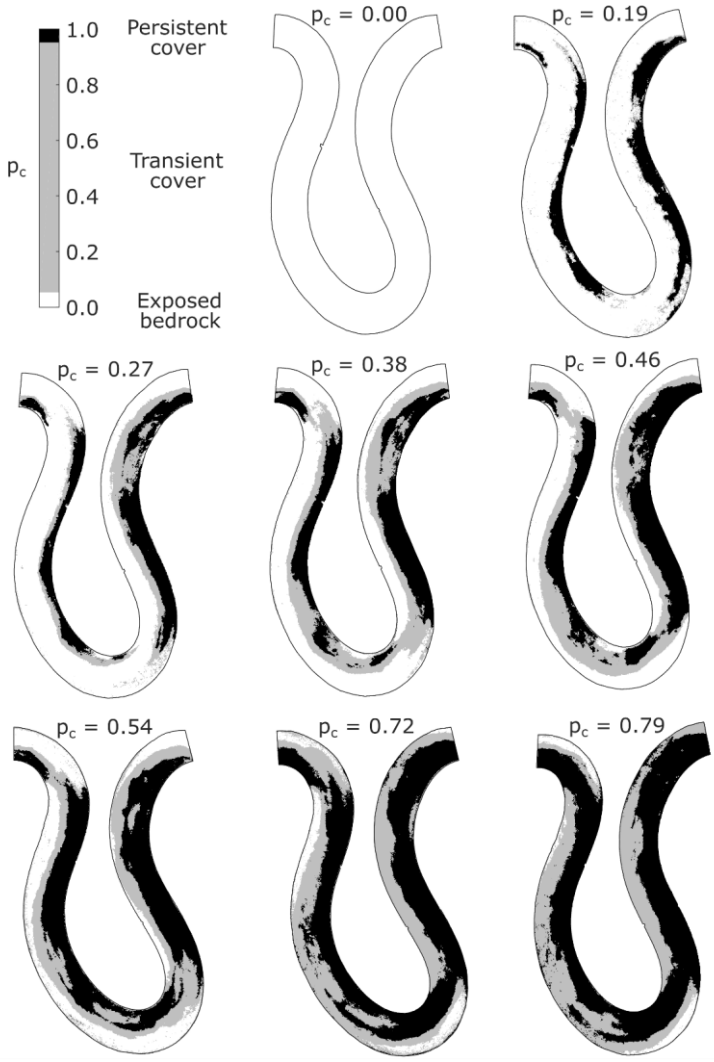

Figure 9 Maps showing regions with persistent alluvial cover, transient alluvial cover and persistently exposed bedrock for all experimental conditions.

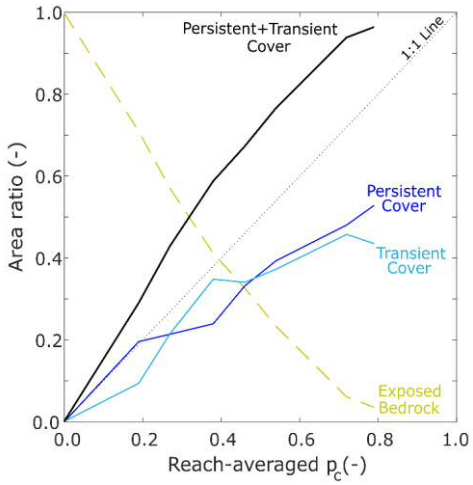

Figure 10 Reach-averaged area ratios of persistently exposed bedrock, transient alluvial cover, persistent alluvial cover, and persistent + transient alluvial cover as a function of reach-averaged areal cover fraction.

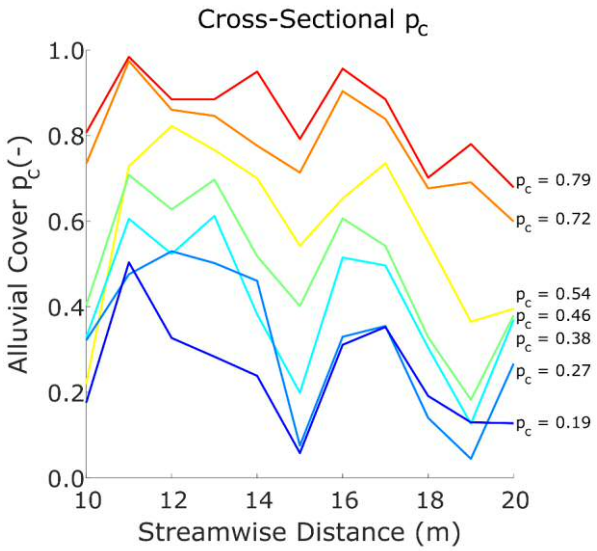

Figure 11 Cross-sectional averages of areal fraction of alluvial cover for all experimental runs. Local values were extracted every meter between streamwise locations 10 m and 20 m. The legend indicates the corresponding reach-averaged values.

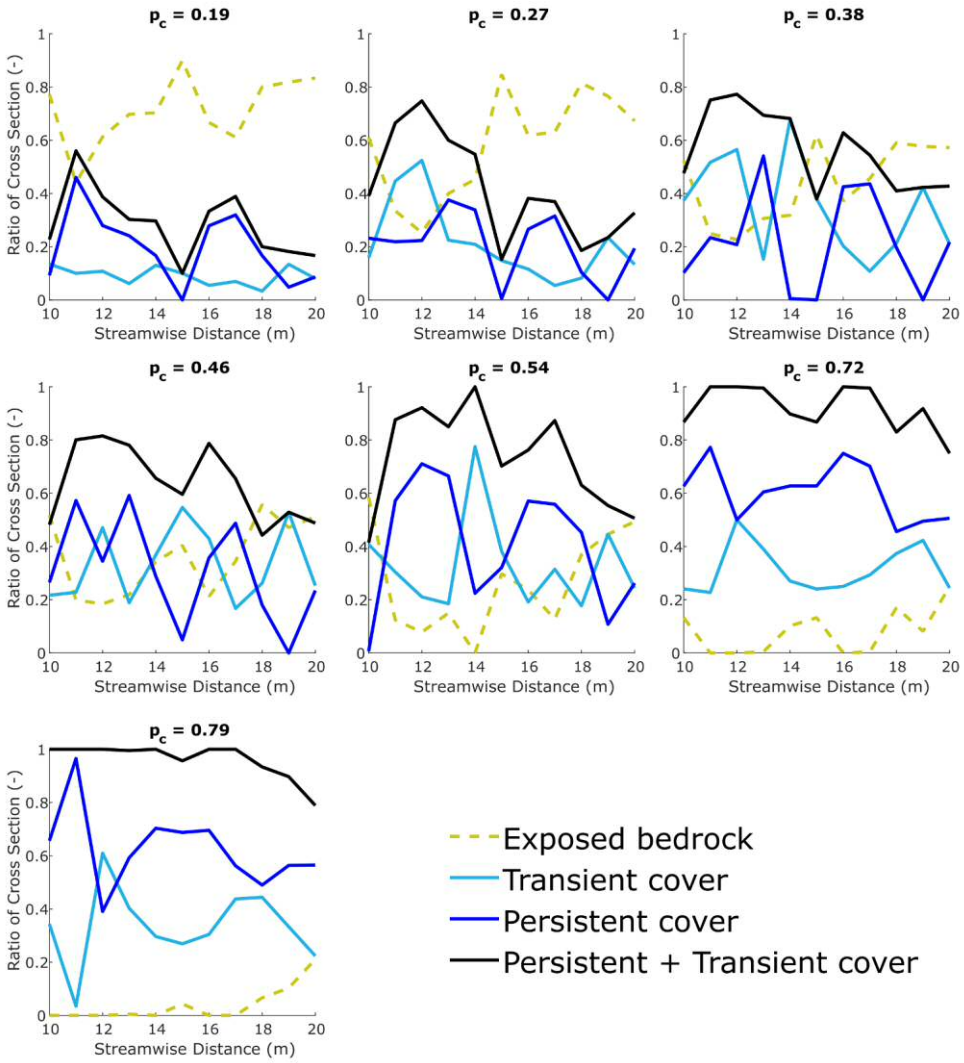

Figure 12 Cross-sectionally-averaged ratios of persistently exposed bedrock, transient alluvial cover, persistent alluvial cover, and persistent + transient alluvial cover for all experimental conditions.

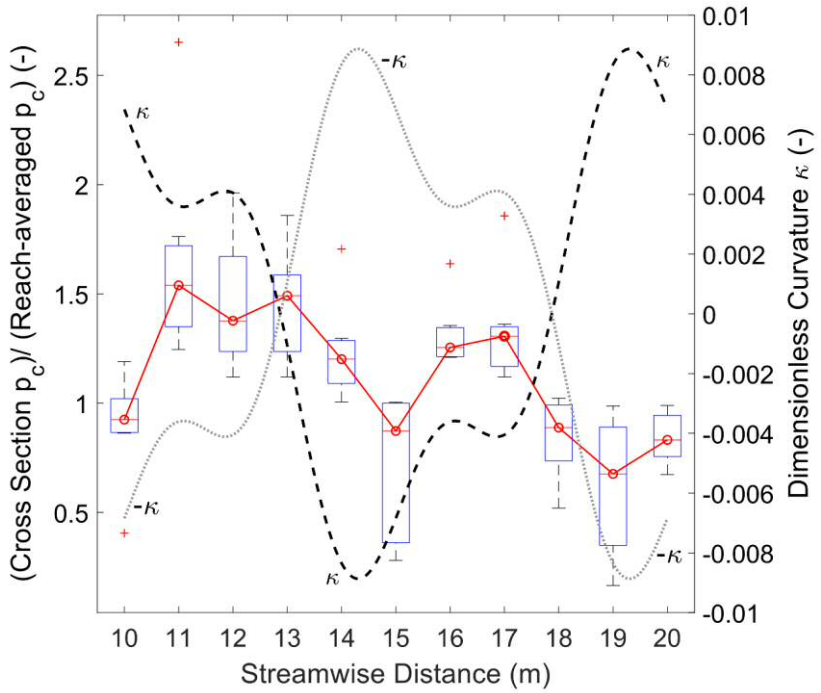

Figure 13 Boxplots of normalized cross-sectionally-averaged areal fraction of alluvial cover in the middle bend of the Kinoshita flume. The dimensionless curvature of the flume κ and its negative value - κ are plotted to better show the salient trends.

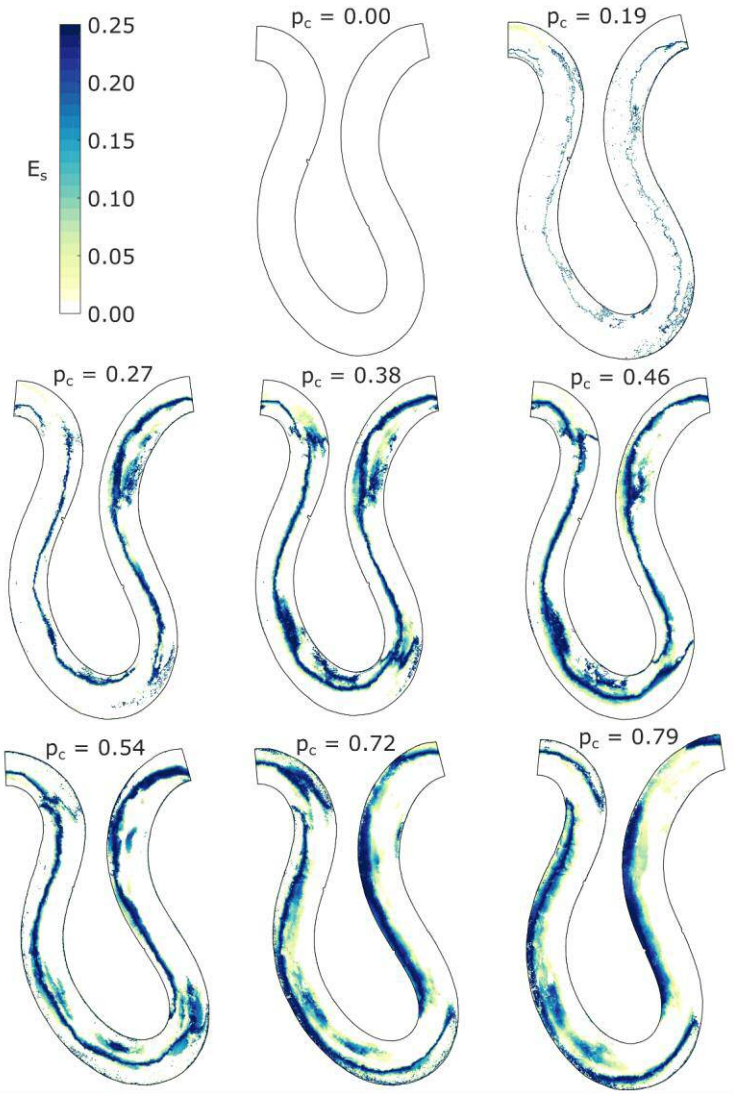

Figure 14 Maps of spatiotemporally-averaged erosion potential for all experimental conditions.

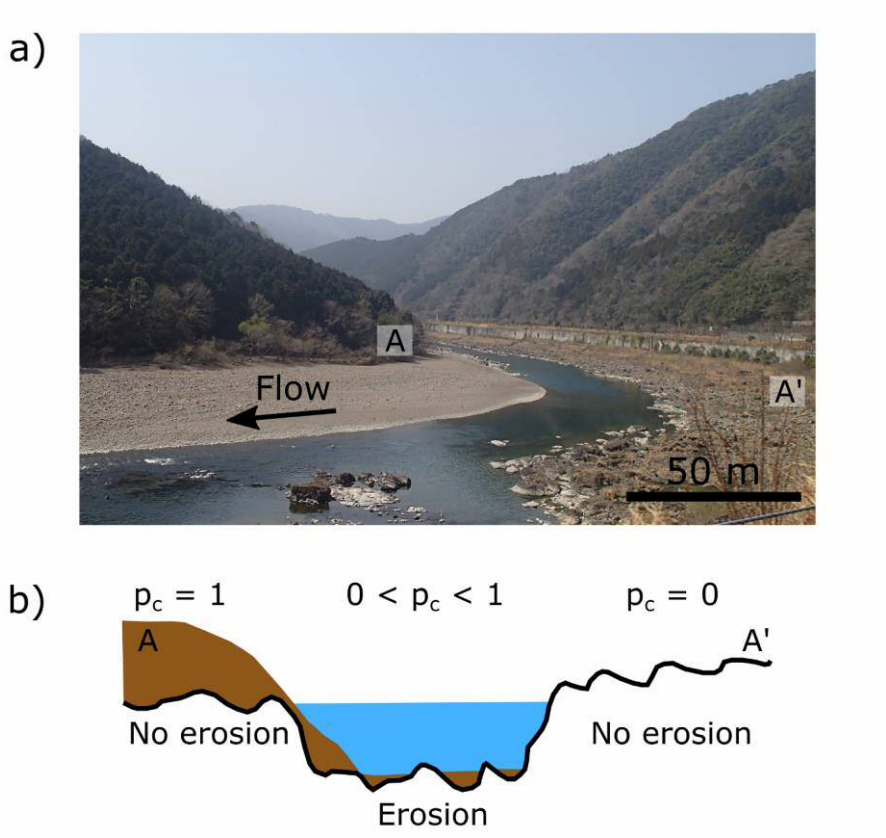

Figure 15 a) Image of a reach of the Shimanto River, Shikoku, Japan showing partial cover with alluvium. b) Sketch of cross section A-A' (with strong vertical exaggeration) indicating inferred regions of erosion and no erosion.

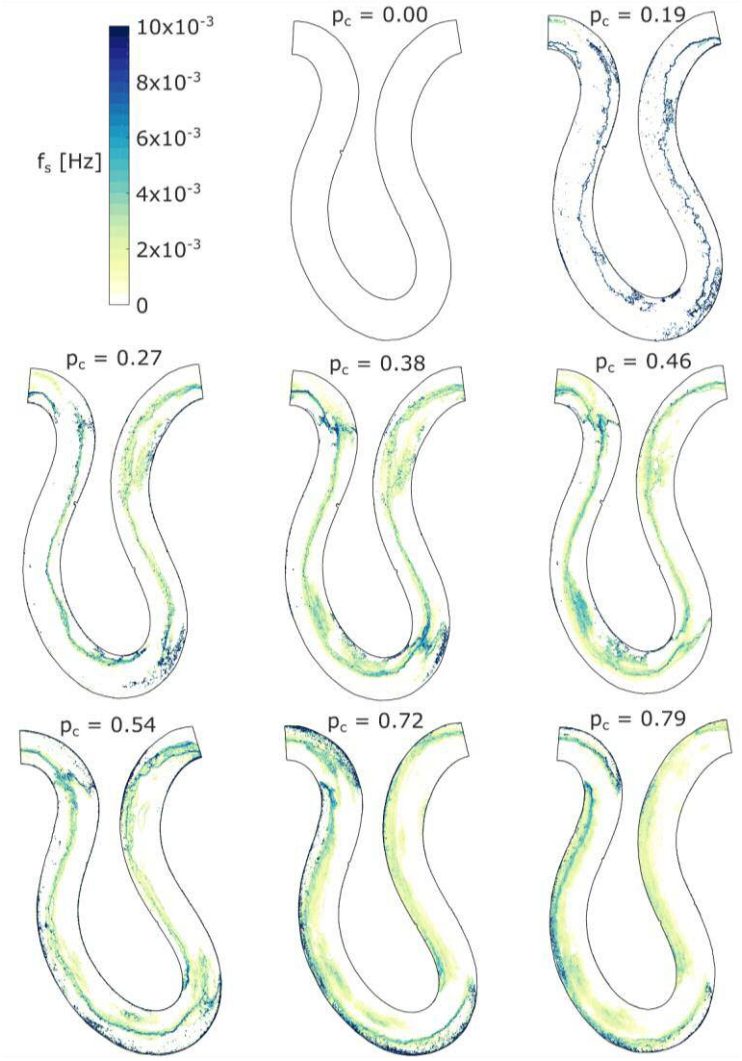

Figure ~~16~~ 15 Maps of frequency of strikes for all experimental conditions. Frequency shown is based on number of images. Dividing the values by 10 s, which is the time between images, will give the actual frequency in Hz.

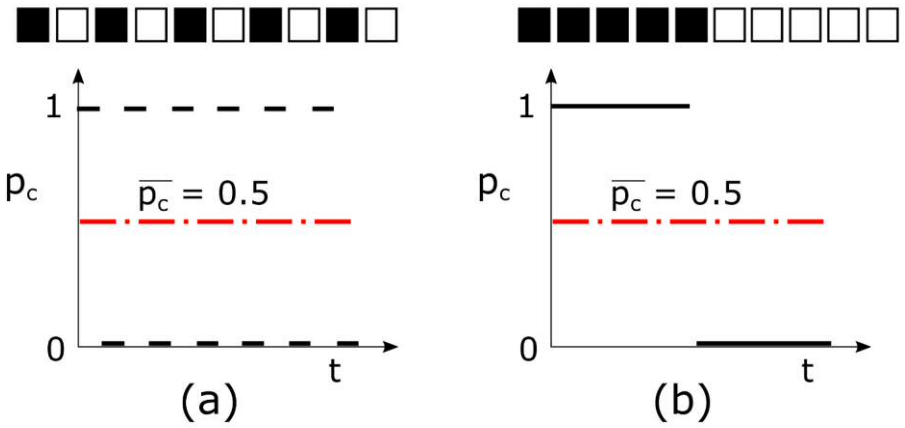

Figure ~~17~~ 16 Simple example showing that temporal averages alone of the areal cover fraction of alluvial cover are insufficient to quantify bedrock incision. Bed conditions (a) and (b) have the same average cover but (a) would experience more erosion than (b) due to a greater frequency of fluctuations in alluvial cover.

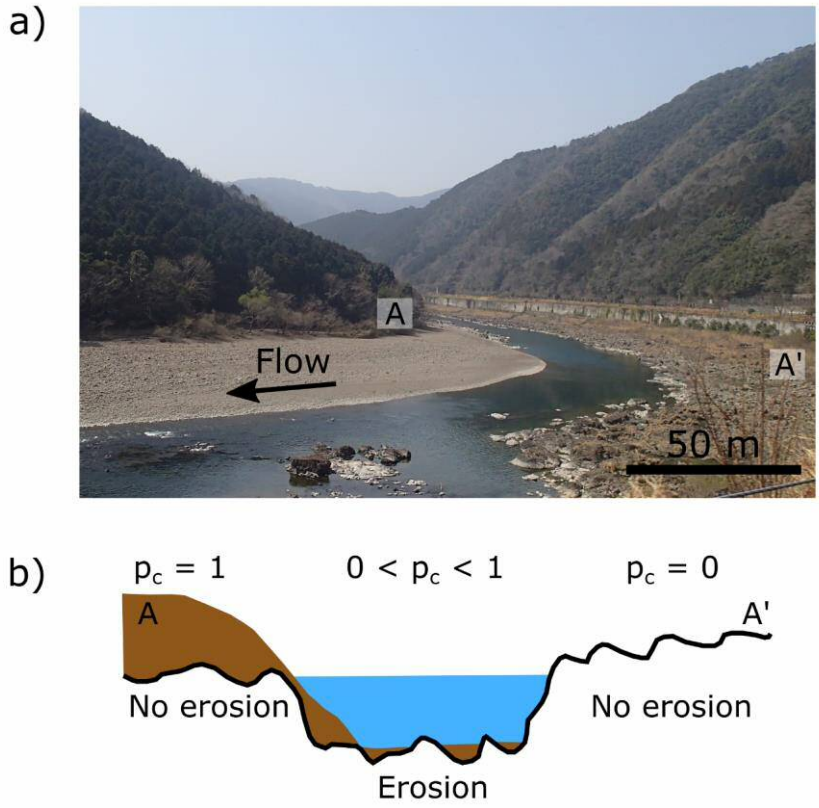

Figure 157 a) Image of a reach of the Shimanto River, Shikoku, Japan showing partial cover with alluvium. b) Sketch of cross section A-A' (with strong vertical exaggeration) indicating inferred regions of erosion and no erosion.